



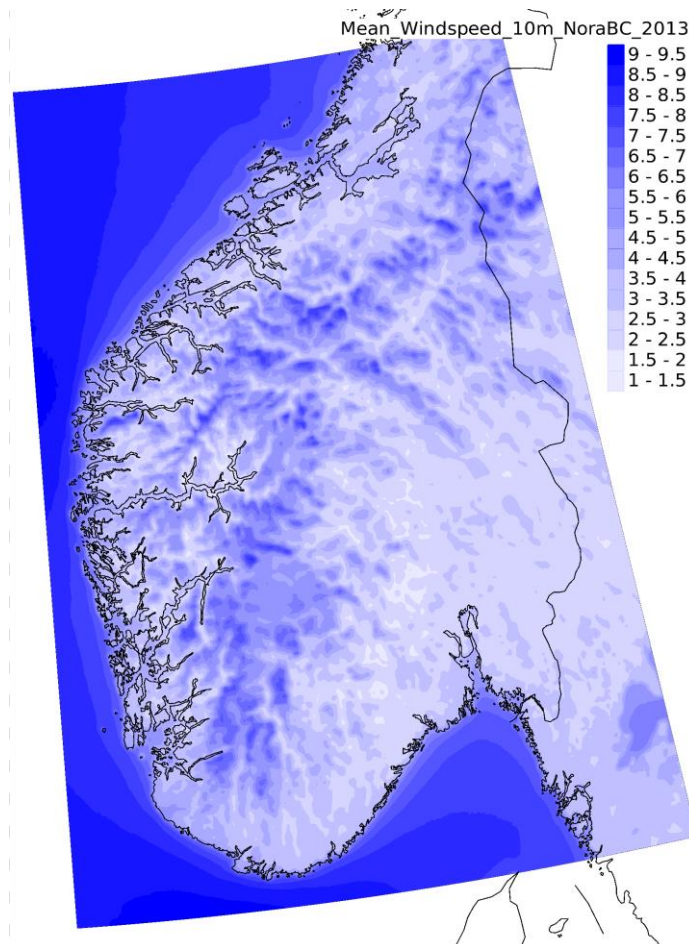
Norwegian
Meteorological
Institute

METreport

No. 5/2017
ISSN 2387-4201
Climate

A 15-year high resolution meteorological dataset for risk assessment in southern Norway.

Haakenstad H. and J.E. Haugen





| | |
|---|---|
| Title A 15-year high resolution meteorological dataset for risk assessment in southern Norway. | Date 2017-02-13 |
| Section Model and Climate Analyse | Report no. No. 5/2017 |
| Author(s) Haakenstad H. and J.E. Haugen | Classification ● Free ○ Restricted |
| Client(s) [Client(s)] | Client's reference [Client's reference] |
| Abstract In this study a 15-year high resolution dataset, NORA-BC, has been produced for risk assessment in southern Norway. The dataset is based on NORA10 which is the best present long-term hindcast for Norwegian areas. NORA10 has been interpolated to a 2.5 km grid and bias corrected with a quantile mapping method, -using the NWP operational AROME data for training. The evaluation of NORA-BC shows that the procedure is able to improve the statistical properties at the local scale, when validated against independent observation based data. The new data set shows less underestimation of strong wind speeds, and too high precipitation rates are reduced. Also 2m temperature shows improvements in the new data set. However, the single parameter quantile mapping method can not retain inter-variable dependencies. | |
| Keywords Hindcast, bias correction, quantile mapping | |

Disiplinary signature

Responsible signature

Abstract

In this study a 15-year high resolution dataset, NORA-BC, has been produced for risk assessment in southern Norway. The dataset is based on NORA10 which is the best present long-term hindcast for Norwegian areas. NORA10 has been interpolated to a 2.5 km grid and bias corrected with a quantile mapping method, -using the NWP operational AROME data for training. The evaluation of NORA-BC shows that the procedure is able to improve the statistical properties at the local scale, when validated against independent observation based data. The new data set shows less underestimation of strong wind speeds, and too high precipitation rates are reduced. Also 2m temperature shows improvements in the new data set. However, the single parameter quantile mapping method can not retain inter-variable dependencies.

Table of contents

| | | |
|----------|---|-----------|
| 1 | Introduction | 9 |
| 2 | Data and method | 11 |
| 3 | Results | 13 |
| 3.1 | Maps | 13 |
| 3.1.1 | 10m Wind speed, figure A.1.1. | 13 |
| 3.1.2 | 2m Temperature, figure A.1.2. | 13 |
| 3.1.3 | 3 hourly Precipitation, figure A.1.3. | 14 |
| 3.1.4 | 2m Relative humidity, figure A.1.4. | 14 |
| 3.1.5 | Surface pressure, figure A.1.5. | 14 |
| 3.2 | Validation against observations | 15 |
| 3.2.1 | 10m Wind speed. | 15 |
| 3.2.2 | Wind direction in 10m above ground level. | 16 |
| 3.2.3 | 2m Temperature | 17 |
| 3.2.4 | 3 hourly Precipitation | 18 |
| 3.3 | SeNorge | 20 |
| 3.3.1 | Snow depth | 20 |
| 3.3.2 | Water saturation in soil | 20 |
| 4 | Conclusion | 21 |
| | Acknowledgements | 22 |
| | Glossary | 23 |
| | References | 24 |
| 5 | Appendix | 26 |
| A1 | MAPS | 26 |
| A2 | Validation against observations | 31 |
| A2.1 | 10m Wind speed | 34 |
| A2.2 | Wind direction in 10m above ground level. | 37 |
| A2.3 | Temperature 2m | 40 |
| A2.4 | Three hourly precipitation | 43 |
| A3 | SeNorge fields | 46 |

List of figures

(See appendix.)

Maps

- Figure A.1.1** 10m wind speed.
a) Mean of NORA-BC (2013).
b) Mean of NORA10 (2013).
c) The difference between AM2.5 and NORA10 (2013).
d) The difference between NORA-BC (2000-2014) and AM2.5 (2013).
- Figure A.1.2** 2m temperature.
a) Mean of NORA-BC (2013).
b) Mean of NORA10-(2013).
c) The difference between AM2.5 and NORA10 (2013).
d) The difference between NORA-BC (2000-2014) and AM2.5 (2013).
- Figure A.1.3** Three hourly precipitation.
a) Mean of NORA-BC (2013).
b) Mean of NORA10 (2013).
c) The difference between AM2.5 and NORA10. (2013).
d) The difference between NORA-BC (2000-2014) and AM2.5 (2013).
- Figure A.1.4** 2m relative humidity.
a) Mean of NORA-BC (2013).
b) Mean of NORA10 (2013).
c) The difference between AM2.5 and NORA10 (2013).
d) The difference between NORA-BC (2000-2014) and AM2.5 (2013).
- Figure A.1.5** Surface pressure.
a) Mean of NORA-BC (2013).
b) Mean of NORA10 (2013).
c) The difference between AM2.5 and NORA10 (2013).

Validation against observations

10m Wind speed

- Figure A.2.1.1** QQ-plot of 10m wind speed.
Figure A.2.1.2 PDF-plot of 10m wind speed.
Figure A.2.1.3
a) Map showing mean values of observed 10m wind speed in the time period 2000 to 2014.
b) Map showing the mean error in the NORA-BC 10m wind speed.
- Figure A.2.1.4** Time series of 10m wind speed for the time period 2000-2014, divided into seasons. Time series are shown for observations, NORA-BC and NORA10. The uppermost figures show the mean value and the lowermost figures show mean error and root mean square error.
a) Winter
b) Spring

- c) Summer
 - d) Autumn
- Figure A.2.1.5** Time series of 10m wind speed percentiles for the time period 1960-2014. Time series are shown for observations and NORA-BC.
- a) 95 percentile.
 - b) 98 percentile.
 - c) 100 percentile.

10m Wind direction

Figure A.2.2.1 Stations selected for wind direction analysis and the wind speed scale colour palette.

Figure A.2.2.2 Wind roses showing observed wind direction, wind direction in NORA-BC and NORA10.

2m Temperature

Figure A.2.3.1 QQ-plot of 2m temperature.

Figure A.2.3.2 PDF-plot of 2m temperature.

Figure A.2.3.3

a) Map showing mean values of observed 2m temperature in the time period 2000 to 2014.

b) Map showing the mean error in the NORA-BC 2m temperature.

Figure A.2.3.4 Time series of 2m temperature for the time period 2000-2014, divided into seasons. The time series are shown for the observations, NORA-BC and NORA10.

The uppermost figures show the mean value and the lowermost figures show mean error and root mean square error.

- a) Winter
- b) Spring
- c) Summer
- d) Autumn

Figure A.2.3.5 Time series of the 98 and the 100 percentile of 2m temperature for the time period 1960-2014. Time series are shown for observations and NORA-BC.

Three hourly Precipitation

Figure A.2.4.1 QQ-plot of 3h precipitation.

Figure A.2.4.2 PDF-plot of 3h precipitation

Figure A.2.4.3

a) Map showing mean values of observed precipitation [daily values/8] in the time period 2000 to 2014.

b) Map showing the mean error in the NORA-BC precipitation.

Figure A.2.4.4 Time series of 3 hourly precipitation for the time period 2000-2014, divided into seasons. Time series are shown for observations, NORA-BC and NORA10.

The uppermost figures show the mean value and the lowermost figures show mean error and root mean square error.

- a) Winter
- b) Spring
- c) Summer
- d) Autumn

Figure A.2.4.5 Time series of daily precipitation for the time period 1960-2014. Time series are shown for observations and NORA-BC.

- a) 95 percentile.
- b) 98 percentile.
- c) 100 percentile.

SeNorge

Figure A.3.1. The figure shows seasonal mean values of snow depth, respectively winter, spring, summer and autumn.

Figure A.3.2. The figure shows seasonal mean values of water saturation in soil, respectively winter, spring, summer and autumn.

List of tables

| | |
|-------------------|--|
| Table A2.1 | Stations used in the analysis of 10m wind speed, 2m temperature and precipitation. |
| Table A2.2 | Stations used in the analysis of long term trends in 10m windspeed. |
| Table A2.3 | Stations used in the analysis of wind direction. |
| Table A2.4 | Beaufort wind scale. |
| Table A2.5 | Wind direction scale. |

1 Introduction

The main objective of the WISLINE-project (Wind, Ice and Snow Load Impacts on Infrastructure and the Natural Environment), funded by the Norwegian Research Council KLIMAFORSK programme, is to quantify climate change impact on technical infrastructure and the natural environment caused by strong winds, icing and wet snow. Two of the sub-objectives are (i) to quantitatively assess future wind and ice design loads on electric transmission lines in different geographical regions in Norway and (ii) to establish risk assessment models for weather hazard induced damages on forests.

The complex topography in southern Norway calls for the need to develop high-resolution datasets able to realistically capture the local variability and quantification of weather parameters like temperature, precipitation and wind. A 1x1km² gridded observation-based dataset for daily temperature and precipitation exist for the Norwegian mainland covering the period from 1957-today (Tveito et al., 1999, Tveito et al., 2000), which recently has been updated (Lussana et al., 2016, Gissnås et al., 2016). Other datasets available by MET Norway are products from the operational numerical weather prediction (NWP) model HARMONIE AROME (Seity et al., 2011) at 2.5x2.5 km² grid, which has been produced since 2013 and cover more parameters including near surface wind, humidity and surface pressure and snow cover. Long-term hindcast data for Norway, NORA10, has been produced on a 11x11 km² grid, based on the NWP model HIRLAM (Reistad et al., 2011 and Reistad et al., 2015) for the period 1958-today. The HIRLAM model was forced by the ERA40 global reanalysis (Uppala et al, 2005) and operational global NWP data from ECMWF IFS model (Andersson, 2015). In addition numerous model-based climate datasets are available from different project coordinating regional downscaling of global climate model experiments, forced by re-analysis data or transient climate change simulations. In the most recent data from EURO-CORDEX (Jacob et al., 2014) the resolution has been improved to 12x12km² grids, which is comparable to the Norwegian hindcast archive, but the time-period covered by re-analysis experiments ends in 2008.

As a remedy for model errors and in order to prepare datasets with statistical properties more comparable to the local observational time series, bias correction methods have been widely used in impact studies and for climate service (Chen et al. 2013, Sorteberg et al., 2014). The correction can take into account different moments or aspects of the data, like mean value, standard deviation, percentiles and extremes. Among the more advanced algorithms, the quantile mapping considers the whole distribution of the parameter to be adjusted, including extremes, so that the corrected data matches the distribution of the training data (or observations) (Thiemeßl et al., 2010, Gudmundsson et al., 2012). The data may be modelled by theoretical distributions (e.g. a normal distribution for temperature or gamma distribution for precipitation or by an empirical approach without specific assumptions about the distribution of the data. Recent studies have compared different RCM bias correction methods. Themeßl et al. (2010) assessed seven bias correction methods used to correct modeled precipitation by the regional climate model MM5 forced with ERA40 reanalysis. They concluded that quantile mapping outperform all methods considered, especially at high quantiles. Gudmundsson et al. (2012) agreed with the above mentioned studies and demonstrated that quantile mapping of the empirical distribution is more suitable in reducing systematic errors in model data.

Sorteberg et al. (2014) tested six distribution-based bias correction methods. They pointed out that all evaluated methods perform reasonably well in i) reproducing statistical properties of the observations including high order moments and quantiles and ii) conserving the climate change signal.

The success of a bias correction procedure is sensitive to several aspects. The calibration period or number of training values will influence the variability of the corrected long-term data and the estimation of extremes, in particular new extremes outside the range of the reference data (Berg et al. 2012). Moreover, when it is applied to correct local conditions, the skill is location dependent (Chen et al., 2013). Themeßl et al. (2012) investigated the transferability of the method to different climate conditions, how well the method reproduces “new extremes” and the impact of quantile mapping on the climate change signal. Furthermore, the internal consistency between model weather parameters is to some extent lost in a single-parameter correction procedure, e.g. link between precipitation and temperature from day to day. Bias correction of a binary variable such as precipitation is also more challenging than bias correction of linear variables such as temperature and wind speed.

The dataset is achieved by a bias correction procedure, using empirical quantile mapping, applied to the Norwegian hindcast data NORA10 for the selected parameters, where the procedure is trained against the high resolution NWP data from the AROME model for year 2013. The result of the training is used to correct the long-term data covering 2000-2014 on a 2.5x2.5 km² grid.

2 Data and method

The dataset should satisfy several needs (i) a relative long-term dataset (2000-2014) for analysis which could be compared to user needs in impact studies, e.g. for forest damage (ii) high temporal and spatial accuracy balanced against available data (3-hourly data at 2.5x2.5km² grid) (iii) relevant spatial coverage (land areas of Southern Norway) (iv) a consistent set of parameters (pressure, 2m temperature and humidity, 10m wind speed, precipitation and snow water equivalent). The basic long-term data is the NORA10 hindcast, but the horizontal resolution of approximately 11 km is relatively coarse for local impact studies. Consequently, the data was adopted to a local grid by comparing the statistical properties to the AROME 2.5x2.5km² reanalysis for the year 2013. A reanalysis includes more observations in the assimilation procedure than an operational run, and it is therefore expected to simulate the weather state even more accurate than an operational weather forecast. All data has been bilinear interpolated to a common 2.5x2.5 km² resolution grid for Southern Norway and bias-corrected using the empirical statistical quantile-mapping method. The quantile mapping (QM) method is distribution-based and corrects for errors in the shape of the distribution. Here, QM is based on point-wise constructed empirical cumulative distribution functions (ecdfs). For a selected parameter, the datasets of AROME and NORA (2.5x2.5km²) are pointwise sorted in increasing order. Then, NORA has been forced to fit the distribution of AROME. The correction function transfers the raw NORA data (X) to the corrected estimate NORA-BC (Y) such that:

$$Y_i^{NORA-BC} = (ecdf_i^{AROME})^{-1} (ecdf_i^{NORA} (X_i^{NORA}))$$

The construction of the empirical cumulative density functions is performed for the year 2013, and NORA is calibrated for the time period 2000-2014. If NORA contains new extremes outside the range of the ecdfs, the same calibration is used as for the uppermost tile in the calibration range.

Temperature, wind speed, precipitation, relative humidity and surface pressure have been processed with the QM method. In addition, liquid water content of surface snow and water saturation in soil have been taken from a separate observation-based product, seNorge (Tveito et al., 1999, Tveito et al., 2000). Although the last two parameters are present in the the hindcast dataset, the long term data showed inconsistencies due to the forcing data, and the alternative seNorge data was selected.

Temperature, wind speed, relative humidity and surface pressure have been bias corrected by using the default quantile mapping method, while precipitation has been handled with a special procedure, using robust empirical quantiles, - where local linear least square regression is used in the estimates of the values of the quantile-quantile relation of AROME and NORA. 100 of the nearest data points are used to apply in the local regression, and 10 bootstrap samples are used in the estimation of the transformation. Wet day correction is also applied. Regarding temperature, samples are confirmed to seasonal time windows, where values within the selected season are used to make the empirical cumulative density functions. When comparing the AROME precipitation to observations, some unrealistic values were detected. So the dataset had to be investigated before it could be used in the QM procedure. In every grid point, AROME was compared to the grid point values of NORA. For every AROME value greater than the grid-point maximum value of NORA, AROME was adjusted by one of the two options:

1. First dividing the AROME precipitation distribution for the specific grid point into 0.1 percent probability intervals by defining:

$$q_i^{AM} = \text{quantiles}(X_i^{AM}, \text{probs} = \text{seq}(0,1,0.001))$$

and modify the AROME –grid point value by performing a reduction of the value based on the 0.6 % upper part of the AROME distribution:

$$X_i^{AM\text{-adjusted}} = q_i^{AM2.5}[995] + (X_i^{AM} - q_i^{AM2.5}[995]) * (q_i^{AM2.5}[998] - q_i^{AM2.5}[995]) / (q_i^{AM2.5}[1001] - q_i^{AM2.5}[995])$$

2. If the adjusted value of AROME [1] is less than the maximum value of NORA in the grid point, the new value of AROME is set to the maximum value of NORA.

3 Results

3.1 Maps

Description of figures A.1.1 to A.1.5 in Appendix.

3.1.1 10m Wind speed, figure A.1.1.

The bias correction of NORA against AM2.5 is clearly affecting the wind speed field in the way that we can expect improvements. The method gives a realistic high resolution version of NORA and the strong variation of the wind speed between the valleys, the mountain slopes and peaks are shown clearly in figure a). Along the fine structure of the coast the wind speed shows an immediately weakening compared to the strong marine values. NORA10 wind speed in figure b) has the coarse field of 11 km horizontal resolution which is insufficient to provide detailed information for land areas. Figure c) shows that the wind speed in AM2.5 is stronger in the mountains compared to NORA10. This is clearly an improvement, since NORA10 has problems with too weak wind speeds in bare mountain areas. NORA10 has a weak overestimation of the mean wind speed in coastal zones (after 2000); (NORA10 Final Report, Figure A1.2 a)), which is corrected due to the weaker coastal wind speed in AM2.5 (figure c). The wind speed in NORA-BC for the period 2000-2014 resemble the AM2.5 field in 2013 (fig d) due to the strong correlation between the mean wind field and the topography. The mean value of the corrected wind field for 2013 in Fig. a) has increased by 0.4 m/s, displaying higher values in the most of the elevated areas in southern Norway.

3.1.2 2m Temperature, figure A.1.2.

The bias corrected and inherent better resolved topography of NORA-BC shows a more realistic 2m temperature field compared to the original NORA10. The differences between AM2.5 and NORA10 are mainly topographically determined; the better resolved topography in AM2.5 shows warmer valleys and fjords and colder mountain peaks compared to NORA10. The warmer valleys are special seen in Ottadalen, Romsdalen and Gudbrandsdalen and the warmer fjords are most clearly seen in the two largest fjords; Sognefjorden and Hardangerfjorden. The averaged bias corrected temperature field for the period 2000-2014 shows mainly colder temperatures than the AM2.5 field for 2013. This may be caused by the anthropogenic warming with lower temperatures in the beginning of the period and higher in the end, however, the year to year variations are so high that it is not possible to prove this suggestion. The strongest difference between 2000 to 2014 and 2013 is seen in the coastal zone stretching a far distance inland. (An area from Trysil and northwards following the boarder between Norway and Sweden shows the opposite picture with colder temperature in 2013 than in the period 2000-2014.)

3.1.3 3 hourly Precipitation, figure A.1.3.

The NORA bias corrected precipitation field has a similar pattern as the normal annual precipitation for Norway (http://www.met.no/English/Climate_in_Norway/), with the wettest areas north of Hardanger fjord to the Møre area. NORA-BC shows values from 0.6 to 1 mm/3hours (~1750 – 3000 mm/year) along the west coast and 1 to 2.2 mm/3H (~3000-6400mm/year) in the mountains, with a local maximum of 2.4 mm/3H at the glacier Alftobreen (or 7000 mm/year). The observed record for the normal period (1961-1990) is 5596 mm a year at Brekke near Sognefjorden (in the county of Sogn og Fjordane). Measurements of annual run-off from glaciers do also indicate that some of the glaciers must have an annual precipitation of about 5000 mm which is also among the highest values in Europe. Østlandet which is geographically placed in the lee areas in relation to the large weather systems coming from west, shows a precipitation rate of 0.2 to 0.4 mm/3H (~500-1000 mm annually). This is also in good agreement with the normal annual precipitation in this area.

NORA10 does also have the same main pattern, with wettest area north of Hardanger fjord to the Møre area and the driest area at Østlandet. NORA10 does also manage to place the extremes; over the glacier Folgefonna, the glaciers Alftobreen and Jostedalsbreen and also where the maximum record has been done south of Sognefjorden. However the maximum value in NORA10 is 1.1 mm/3H (~3200mm annually) and the finer topographic details are lacking.

Figure c) shows the difference between AM2.5 and NORA10. NORA10 shows higher precipitation rate than AM2.5 in the mountains from Setesdalsheiene (inland Boknafjorden which is south of the Hardangerfjord) in south to Trollheimen and Dovrefjell (on the border of the counties Møre og Romsdal, Trøndelag and Oppland) in the north. AM2.5 shows higher precipitation rate for glaciers and also but in less degree in the coastal zone.

Figure d) shows the difference between NORA-BC (time period 2000-2014) and AM2.5 in 2013. NORA10-BC shows a drier field in the mountain and a wetter field especially in south-western Norway but also at the lee side of the mountains and in Sør-Trøndelag county.

3.1.4 2m Relative humidity, figure A.1.4.

Figure a) shows a relative humidity field having a general value between 0.8 and 0.9. Some places are more dry, as over the fjords at Vestlandet and parts of Østlandet (values below 0.8, and some few areas below 0.75). The coast of the northern-part of Vestlandet has also low relative humidity. The maximum values are limited to the mountains. The low relative humidity over fjords and at the coast of northern Vestlandet can probably be explained by the higher temperatures in these areas compared to the temperatures above the ambient land surface with the steep topography. In the mountains the cold temperatures contribute to high relative humidity.

Figure b) shows that NORA10 has the same pattern as NORA-BC; with low relative humidity over the fjords and at the coast of northern Vestlandet and high values in the mountains. Figure c) shows that the NORA10 does not have as high values as AM2.5 in the mountains, and not as low values as AM2.5 elsewhere. Figure d) shows that NORA-BC for the time period 2000-2014 has lower relative humidity over the whole area compared to AM2.5 in 2013.

3.1.5 Surface pressure, figure A.1.5.

Figure A.1.5 a) shows the NORA-BC field of surface pressure. The surface pressure is mainly predefined by the topography, with decreasing values with height due to the thinner air. Figure b) shows the surface pressure field of NORA10, which has the coarser resolution and is lacking the topographical details. This shows up in figure c); with higher surface pressure in the better resolved valleys of AM2.5 and less surface pressure at the mountain peaks.

3.2 Validation against observations

In the validation against observations, the station list in table A2.1 has been used. The model values have been bilinear interpolated to the observation points.

3.2.1 10m Wind speed.

Figure A.2.1.1 shows the qq-plot of 10m wind speed. The quantile values of NORA-BC, NORA10 and AM2.5 for year 2013 are compared to observations. NORA-BC has been pushed against the AM2.5 which has values matching better to the observations than NORA10. All the models are underestimating the strongest wind speeds. NORA10 underestimate wind speeds stronger than about 8 m/s while AM2.5 and NORA-BC are underestimating wind speeds stronger than about 15 m/s. Maximum values in the NORA10 is 28.1 m/s, in NORA-BC 28.2 m/s, in AROME 28.5 and in the observations 36.8 m/s. The observed values show 19 values above 28.2 m/s out of a sample of 251876 observed values. In other words, NORA-BC is lacking the 0.0075% strongest observed wind speed values.

Figure A2.1.2 shows PDF plot of 10m wind speed. AM2.5 and NORA-BC have PDFs matching very good to the PDF of the observations. NORA10 shows a strong overestimation of cases with light and gentle breeze. Fresh breeze and cases with stronger wind speed are underestimated in NORA10. All the models underestimate calm and light air, but AM2.5 and NORA-BC match very well with the upper tail of the wind distribution. So the underestimating of the highest wind speeds shown in the QQ-plot (fig A2.1.1) is not visible in the PDF because of the rare happenings of these wind speeds.

Figure A.2.1.3 a) shows mean values of observed 10m wind speed in the time period 2000 to 2014 on the map. (Overlapping stations on the map are removed to make the figure readable, however, all the stations are used in the calculations of the models performances.) Strongest wind speeds are shown on the west coast; with Kråkenes light house having a mean wind speed of 8.5 m/s. Utsira does also show a mean value above 8 m/s. Inland, Juvasshøe has the strongest mean wind speed of 7.7 m/s. East of the mountains, the mean wind is much lower, typically below 2.5 m/s. Figure 2.1.3 b) shows that this values are typically overestimated in NORA-BC.

Figure A.2.1.3 b) shows mean error in the NORA-BC wind speed on the map. There is a weak majority of overestimated values in the NORA-BC wind speed. The overestimation is mainly concerning stations having relatively weak mean wind speeds and the mean overestimation is 0.7 m/s. Underestimation of the mean wind is mainly concerning stations nearby the coast or mountain stations and the mean underestimation is of 0.5 m/s.

Figure A.2.1.4 shows time series of 10m wind speed for the time period 2000 to 2014. The time series show observations, NORA-BC and NORA10. (The values are mean values of all the stations and all time steps in a season.) The model wind speed is overestimated in the winter and autumn, while the mean error is almost zero in spring and summer. The overestimation of the wind speed in winter and autumn is approximately of 0.5 m/s in both NORA10 and NORA-BC and is relatively stable during the time period 2000 to 2014. While the bias corrected data is not outperforming NORA10 in mean error, the root mean square error is slightly lower in NORA-BC. There is a negative trend in the mean observed wind speed over the period 2000-2014, while the extreme values (the maximum) show a positive trend (fig A2.1.5). However, the year to year variations are relatively high, so the time period of 15 years is somewhat too short time to establish certain long term-trends.

Figure A.2.1.5 shows time series of the 95, 98 and 100 percentiles of 10m wind speed for the time period 1960 to 2014. Because of large year to year variations in extremes, it is not possible to establish meaningful trend values for the period 2000 to 2014. Therefore, observations are shown for the long term time period 1960 to 2014 while the NORA-BC are shown for the shorter time period 2000 to 2014. The time series are just based on 19 stations, with the intention to operate with a homogeneous station list over the whole time period 1960 to 2014 (table A2.2). The observations show increasing trend in wind speed for these uppermost percentiles; the observational trend in the 95 percentile wind speed is 0.0078 m/s/year. Starting from a mean value of 11.5 m/s, this trend will result in a mean value of 11.9 m/s after 55 years. The observational trend in the 98 percentile wind speed is 0.015m/s/year. This trend means an increase from 13.9 m/s to 14.8 m/s in 55 years. The observational trend in the 100 percentile wind speed is 0.16 m/s/year, which gives an increase from 27.8 m/s to 36.6 m/s in 55 years.

3.2.2 Wind direction in 10m above ground level.

11 stations given in table A2.3 are selected to present the bias corrected wind direction. The stations are geographically dispersed in the WISLINE domain (see figure A2.2.1), and the wind direction is shown in wind roses (see figure A2.2.2). Table A2.4 shows the wind direction scales.

a) Gardermoen

The most common wind direction at Gardermoen is from south and second most common from north-north-east. Both NORA-BC and NORA10 have correct main direction, but the bias corrected wind direction has even more cases from south, which match very good to the observations. NORA-BC has the second most common direction from north, while the observation shows a second most common direction from north-north-east. The bias corrected wind direction has also more calm situations, although the calm situations are largely underestimated. Cases with wind from west are reduced in the bias corrected wind directions in good agreement with the observations.

b) Røros

The most common wind direction at Røros is from north-north-west. Wind directions from south-south-west and south – south-east are also common. Røros has also many calm situations, which is absent in NORA10. NORA-BC has some calm situations, but they are still largely underestimated. NORA10 overestimate situations with wind direction from south.

c) Kvitfjell

The most common wind directions at Kvitfjell are from south and from north-north-west. The bias corrected wind direction shows an overestimation of cases with wind direction from south. The number of cases with wind direction from north-north-west were better predicted in NORA10. NORA10 has an overestimation of wind direction from south-south-east, while the observations rather show wind direction from south.

d) Grotli III

The most common wind directions at Grotli are from north-north-west and from west and from east. NORA-BC shows a wind rose matching much better the wind rose of the observations compared to NORA10 which has an overestimation of the cases with wind direction from south, south-south-west and south-south-east. Calm situations are quite few, -also in the observations.

e) Rygge

The most common wind direction at Rygge is from south and then from north. NORA-BC has a wind rose matching very well the wind rose of the observations. NORA10 has also a well matching wind rose, but is outperformed of the NORA-BC.

f) Ferder lighthouse

Also at Ferder light house NORA10 and NORA-BC show a well match of the wind directions to the observations, but except for the direction north-north-east, NORA-BC outperforms NORA10 in matching the observations. The calm situations are almost absent, -also in the observations.

g) Utsira lighthouse

Utsira lighthouse has no observed calm situations in 2013. The observed main wind direction is from south, then from south-south-east, and wind direction from north is also common. NORA-BC has a well matching wind rose to the observations. NORA10 shows also well estimated wind directions, but with an underestimation of wind directions from north and an overestimation of situations with wind directions from south.

h) Flesland

The main observed wind direction at Flesland is from south-south-east. NORA-BC has improved the number of situations with wind direction from south, south-south-east and north. NORA10 overestimates situations with wind direction from south, underestimates situations with wind directions from south-south-east and from north.

i) Ytterøyane lighthouse

The main wind direction at Ytterøyane lighthouse is from south. The wind rose of NORA-BC and NORA10 is well matching the observation, but there are 409 observed calm registrations, which is absent in NORA10 and almost also absent in NORA-BC (just 4 cases).

j) Svinøy lighthouse

The main wind direction at Svinøy lighthouse is from south-south-west. Both NORA-BC and NORA10 have an overestimation of wind direction from south and from north-north-east. The bias correction has not introduced significant improvements for this station.

3.2.3 2m Temperature

Figure A.2.3.1 shows the qq-plot of 2m temperature. The figure shows that NORA-BC and AM2.5 provide better maximum values of 2m temperature than NORA10. NORA-BC has the best match to the observations for low temperatures, and approximately as good as AM2.5 for high values. Temperatures in the interval -15°C to $+15^{\circ}\text{C}$ match well to the observations for all the three models. NORA10 underestimates temperatures below approximately -15°C and also temperatures above approximately 15°C .

Figure A2.3.2 shows the PDF of 2m temperature. In contrast to the qq-plot in which the differences in extremes are clearly displayed, the differences in the main part of the distribution emerge more clearly in the PDF plot. The PDF shows an observation range of -39 to 31°C . There are no big differences between the models, and all the three models follow the observation distribution quite well. NORA-BC performs somewhat better for temperatures in the range -13 to -9°C , and in the range 5 to 11°C . AM2.5 performs somewhat better for temperatures in the range 3 to -8°C .

Figure A.2.3.3 a) shows the mean value of observed 2m temperature in the period 2000-2014. The temperature range between -3.4 to 8.8°C for the different stations. The mountain stations; Mannen, Hjerkin, Finsevatn, Grotli, Juvasshøe, Filefjell and Sognefjell have negative mean values. Juvasshøe has the coldest mean temperature of -3.4°C . Coastal stations have typically a mean temperature above 8°C , with Slåtterøy lighthouse, Lindesnes lighthouse and Ferder lighthouse with the highest temperatures. The mean value for all the stations is 5.1°C .

Figure A.2.3.3 b) shows the mean error in the NORA-BC temperature. The bias corrected temperature is mainly underestimated at most stations; in average with -0.39°C . Largest deviation from observation is at Tafjord with mean error of -4.3 and Mannen with 2.1°C .

Figure A.2.3.4 shows time series of 2m temperature for the time period 2000 to 2014. The time series show observations, the bias corrected NORA and NORA10. (The values are mean values of all the stations and all time steps in a season). The uppermost figures show the mean value and the lowermost figures show mean error and root mean square error.

Winter

Mean value for the winter season is -2.11°C . The time series starts with an abnormal warm winter in 2000, with min and max values for the selected stations ranging between -26.0 to 15.0°C (this values are taken out of the r-script reading the observations) and a mean value of 0.2°C , which is 2.3°C warmer than the mean value for the period. The winter 2010 was abnormal cold with a mean value of -8.3°C , (then 6.2°C colder than the mean) and temperature ranging between -40.7 to 5.8°C (the temperature range is not shown in the figure, but is just output from the r-script reading the observations).

Regarding the performance of NORA10 and NORA-BC; they both perform well. However, the models underestimate the winter temperatures for most of the winter seasons. The underestimation is significantly less in NORA-BC (average mean error is -0.17°C) than in NORA10 (having an average mean error of -0.35°C). The average root mean square error of NORA-BC is 2.14°C and 2.37°C for NORA10.

Spring

The mean value of the spring season is 4.3 °C. The coldest observed spring mean is 2.4 °C in 2013 and the warmest is 5.7 °C in 2014 (showing the strong variations between the different years). Observations are ranging between -28.5 and 23.8 °C, with the coldest temperature in 2001 and the warmest in 2012 (also taken from the r-script).

Also in the spring season, the models underestimate the temperature. The time series of NORA-BC is much closer to the observations than NORA10 and has lower mean error and root mean square error.

Summer

The mean value of the summer season is 13.6 °C. The lowest mean value is 12.0 °C and occurred in 2000 and the highest mean value is 15.2 °C which occurred in 2002. The observed range of values for the summer season is -8.2 to 27.4 °C, where the minimum value happened in 2012 and the maximum in 2014.

Also the summer mean values of temperature are somewhat underestimated by the models. NORA-BC performs much better than NORA10, with an averaged mean error of -0.25 °C compared to -0.56 for NORA10. The average root mean square error is also less for NORA-BC (1.22 °C) compared to NORA10 (1.43 °C).

Autumn

The mean value of the autumn season is 6.1 °C. The lowest mean value is 3.5 °C occurring in 2010. The highest mean value is 8.2 °C occurring in 2006. The observed range of values for the autumn season is -29.35 to 22.73 °C, where the minimum value occurs in 2010 and the maximum value occurs in 2005.

The models underestimate the temperature also for the autumn season. It is no big differences in the performance of the models, but NORA-BC is slightly better than NORA10 having an average mean error of -0.4 °C, compared to -0.45 °C for NORA10. The average root mean square error is also somewhat less in NORA-BC (1.4 °C) compared to NORA10 (1.53 °C).

Figure A.2.3.5 shows time series of the 98 and 100 percentile of 2m temperature for the time period 1960-2014. In the situation of an already advanced anthropogenic warming in 2000 and large inter annual variations it is not meaningful to just look at temperature trends for the period 2000 to 2014. In this case we look at the observations for the time period 1960 to 2014 to smooth out the inter-annual variations. The figure shows a trend in the 98 percentile of temperature of 0.02 °C/year resulting in an increase from 19.5 to 20.6 °C in 55 years. The trend in the 100 percentile is 0.06 °C/year resulting in an increase from 28.1 to 31.4 °C in 55 years.

3.2.4 Three hourly Precipitation

Figure A2.4.1 shows the qq-plot of 3 hourly precipitation for the models NORA-BC, NORA10 and AM2.5 in 2013. (The datasets are divided into 1001 percentiles. All values are used. 45 % of the observed values are zero.)

NORA10 underestimates precipitation rates above 2 mm/3h, NORA-BC and AM2.5 just underestimate the uppermost percentile. The maximum value of the observations is 13.1 mm/3H while the maximum values in the models; NORA10, NORA-BC and AM2.5 are respectively 10.0, 10.3 and 10.6 mm/3H.

Figure A2.4.2 shows the PDF of 3 hourly precipitation. (All values below 0.01 mm/3H are removed from the datasets). The PDF of 3 hourly precipitation shows 37% observed precipitation in the interval 0.01 to 0.1 mm/3H, approximately 55 % of the observed precipitation occur in the interval 0.1 to 2 mm/3H, while frequencies above 2.0 mm/3H constitutes less than 10 % of the precipitation. However it is the rare high values which are of most interest, and NORA-BC and AM2.5 seems to match the observations better than NORA10 in the uppermost tail of the distribution.

Figure A2.4.3 a) shows the mean values of 3 hourly precipitation in the time period 2000 to 2014 on the map. The mean observed precipitation frequency is 0.35 mm/3H. Stations observing the highest precipitation rates are Takle (1.1mm/3H), Ualand-Bjuland (0.9 mm/3H), Bergen, Flesland and Førde (0.8 mm/3H). Least precipitation is observed at Evenstad (0.13 mm/3H), Hjerkins (0.14 mm/3H) and Tynset (0.14 mm/3H).

Figure A2.4.3 b) shows the mean error in the NORA-BC precipitation rate compared to observations.

NORA-BC shows best performance for the stations Kvamsøy (ME of -0.006 mm/3H), Lista (0.006 mm/3H), Melsom and Ferder Lighthouse (0.009 mm/3H). NORA-BC shows least performance for the stations Finsevatn (0.45 mm/3H), Tafjord (0.38 mm/3H) and Ytterøyane Lighthouse (0.31 mm/3H).

Figure A.2.4.4 shows time series of precipitation for the time period 2000 to 2014. The time series show observations, NORA-BC and NORA10. (The values are mean values of all the stations and all time steps in a season). The uppermost figures show the mean value and the lowermost figures show mean error and root mean square error.

Winter

Daily observations of precipitation are divided into 3 hourly precipitation rates to be compared with the model data. The mean value of the observations in the winter season is 0.39 mm/3H. The lowest mean value is 0.15 in 2010 and the highest value is 0.48 in 2000. When looking at the single observations, the maximum value is 14.7 mm/3H in 2009 and the minimum of all the winter maximum values occurred in 2010 and was 4.8 mm/3H. (These values are not shown in the figure.)

NORA-BC has mean values matching better to the observations than NORA10 and an average mean error of 0.12 mm/3H compared to NORA10 0.16 mm/3H. The root mean square errors are almost the same.

Spring

Except for the year 2000, the spring mean values are low in the first years of the period, but increases after 2006. The mean value of the observations in the spring season is 0.26 mm/3H, minimum seasonal mean value took place in 2004 (0.22 mm/3H) and maximum seasonal mean value took place in 2000 (0.32 mm/3H). The maximum value observed was 12.9 mm/3H and occurred in 2012. Minimum value of the seasonal maximum values was 5.3 mm/3H and occurred in 2006 (-not shown in the figure).

NORA-BC has mean values with a better match to the observations than NORA10. The average mean error of the NORA-BC precipitation is 0.06 mm/3H, while NORA10 has an average of 0.12 mm/3H. The average of the root mean square error is the same for the two models 0.41 mm/3H.

Summer

The mean observed summer precipitation frequency is 0.37 mm/3H. The maximum of the summer mean values is 0.54 and the minimum is 0.28 mm/3H. The maximum occurs in 2011 and the minimum in 2006. It is a steady increase in the mean precipitation frequency for the summer season from 2006 to 2011. The years 2012 to 2014 shows average precipitation rates.

The maximum value observed in the summer season was 13.2 mm/3H and occurred in 2014. Minimum value of the seasonal maximum values was 7.1 mm/3H and occurred in 2003 (-not shown in the figure). The mean errors in NORA-BC and NORA10 are almost the same until 2012, when NORA-BC performs better than NORA10 for the last three years. The average mean error is 0.06 for NORA-BC and 0.07 for NORA10. NORA10 shows a lower root mean square error of 0.60 compared to NORA-BC 0.64 mm/3H.

Autumn

The mean observed autumn precipitation frequency is 0.46 mm/3H. The maximum of the summer mean values is 0.63 and the minimum is 0.34 mm/3H. The maximum occurs in 2000 and the minimum in 2002. The maximum value observed in the autumn season was 40.2 mm/3H and occurred in 2010.

Minimum value of the seasonal maximum values was 9.3 mm/3H and occurred in 2001 (-not shown in the figure).

There are small differences between the performance of NORA-BC and NORA10. NORA-BC has an average mean error of 0.10 while the average mean error of NORA10 is 0.12. The average root mean square error is 0.59 for NORA-BC and 0.58 for NORA10.

Figure A.2.4.5 shows time series of the 95, 98 and 100 percentile of daily precipitation for the time period 1960-2014. For the same reason as in chapter 3.2.1 and 3.2.3, we look at the long term trend 1960-2014 to establish a more reliable trend for daily precipitation than we would get from the shorter time period 2000 to 2014. The figure shows the trends in daily precipitation of 0.02 mm/day/year for the 95 percentile, 0.03 mm/day for the 98 percentile and 0.1mm/day/year for the 100 percentile.

3.3 SeNorge

3.3.1 Snow depth

The models, NORA10 and AM2.5 are forced with unrealistic high snow depth values and it shows up that the snow output from NORA10 is unrealistic. AM2.5 solves this problem by assimilating observations into the model. NORA10 does not correct for the snow error, because it is running without data assimilation, and allows snow to accumulate until it melts in the spring. This causes unrealistic values not suited for bias correction. Instead of delivering snow depth from the models, we have retrieved the seNorge-snow fields, and converted them to the WISLINE domain. The format of the snow depth is converted from binary to netcdf. Figure A.3.1 shows seasonal mean fields of seNorge snow depth. The spring season has the highest values, with more than 500 cm snow depth in the mountains.

3.3.2 Water saturation in soil

Since water saturation in soil is not a standard output from the models, we use seNorge-fields for this parameter. Binary fields are downloaded from SeNorge, and converted to netcdf and to the WISLINE domain. The mean fields for the different seasons are displayed in figure A.3.2.

4 Conclusion

The NORA10 hindcast is our best present long-term hindcast with available parameters requested for the projects and with sub-daily coverage. For adaptation to the high-resolution grid, the AROME data provide the best consistent model-based product with known qualities as operational weather prediction model suitable for training data. The evaluation of the 3-hourly data after quantile mapping included independent observational data for wind speed, temperature and precipitation. Different statistical measures; quantiles, probability density functions, annual variability and spatial distributions of the error were included. In addition to the internal validation of the correction method, we found that the procedure is able to improve the statistical properties at the local scale, when validated against independent observation based data. The quantile mapping method used in this study has provided a high resolution data set with better performance than NORA10. The underestimation of strong wind speeds and high precipitation rates is reduced. Also 2m temperature shows improvements in the new data set. However, the single parameter quantile mapping method can not retain intervariable dependencies. There is also a risk of adding artificial variability to the parameters (*White and Toumi, 2013*). The data set should be used with caution if forcing other models.

When analyzing the climate change impact in this study, we should have in mind that 2000- 2014 reflect a time period when the global warming already has been ongoing for several decades. In the Arctic the warming has just been accelerating. For the Norwegian mainland, all the 15 years studied here show mean temperatures above the normal. An exception is 2010, which showed continental mean temperature below normal due to very stable weather systems in line with typically systems for the past climate.

Acknowledgements

We are thankful to Lise Seland Graff who provided the AROME data. We want to thank Harold Mc Innes for theoretical feedback to this report and Svein Solberg at the Norwegian Institute of Bioeconomy Research (NIBIO) who was the pilot user of the NORA-BC data. We acknowledge the Norwegian Research Council for the funding of the WISLINE project.

Glossary

| | |
|---------|---|
| AROME | A convective scale numerical weather prediction model. AROME is the abbreviation of “The Application of Research to Operations at Mesoscale”. AROME is used in the Scandinavian operational weather prediction system, AROME-MetCoOp. From November 2016 a newer version of AROME is used in an ensemble system, MEPS. |
| AM2.5 | AROME-MetCoOp operational run with 2.5 km horizontal resolution. |
| ECDF | Empirical Cumulative Density Function |
| ECMWF | European Centre for Medium-Range Weather Forecasts |
| ERA40 | A re-analysis of meteorological observations from September 1957 to August 2002 produced by ECMWF. |
| HIRLAM | High Resolution Limited Area Model which served as the operational weather prediction model in Norway in the years 1995-2014. The HIRLAM member states were Denmark, Finland, Iceland, Ireland, Netherlands, Spain, Sweden and Norway. |
| NORA10 | A hindcast archive for Scandinavian areas produced at MET by running the numerical weather prediction model HIRLAM forced by ERA40 and ECMWF operational analysis. The time period is from September 1957 and the horizontal resolution is approximately 10 km. |
| NORA-BC | NORA10 interpolated to a 2.5 km grid and bias corrected with a quantile mapping method using the NWP operational AROME data for training. |
| QM | The bias correction method, quantile mapping. |

References

Andersson, 2015, *User guide to ECMWF forecast products*

Berg, P., H. Feldmann, and H.-J. Panitz (2012), *Bias correction of high resolution regional climate model data*, *J. Hydrol.*, 448–449, 80–92, doi:10.1016/j.jhydrol.2012.04.026

Chen, J., F. P. Brissette, D. Chaumont, and M. Braun, (2013), *Finding appropriate bias correction methods in downscaling precipitation for hydrologic impact studies over North America*. *Water Resources Research*, Vol. 49, 4187-4205, doi: 10.1002/wrcr.20331.

Gisnås, K., B. Eitzelmüller, C. Lussana, J. Hjort, A. B. K. Sannel, K. Isaksen, S. Westermann, P. Kuhry, H. H. Christiansen, A. Frampton, J. Åkerman, 2016, *Permafrost Map for Norway, Sweden and Finland, Permafrost and Periglacial Processes*, DOI: 10.1002/ppp.1922

Gudmundsson, L., Bremnes, J. B., Haugen, J. E. and Engen Skaugen, T., (2012), *Technical Note: Downscaling RCM precipitation to the station scale using quantile mapping – a comparison of methods*, *Hydrology and Earth System Sciences Discussions.*, 9, 6185-6201. doi:10.5194/hessd-9-6185-2012.

Jacob, D et al. (2014): *EURO-CORDEX: new high-resolution climate change projections for European impact research*. *Regional Environmental Change*, Volume 14, Issue 2, pp 563-578.

Lussana C., O. E. Tveito, F. Uboldi, 2016, *seNorge v2.0: an observational gridded dataset of temperature for Norway*, METreport 14/2016. ISSN 2387-4201, *Climate*.

Reistad, M., Ø. Breivik, H. Haakenstad, O. J. Aarnes, B. R. Furevik, and J. Bidlot (2011), *A high-resolution hindcast of wind and waves for the North Sea, the Norwegian Sea, and the Barents Sea*, *J. Geophys. Res.*, 116, C05019, doi:10.1029/2010JC006402.

Reistad M, H. Haakenstad, B. Furevik and J. E. Haugen .(2015) *NORA10 - Final report 2015. The atmospheric part*. *Norwegian DeepWater Programme – report*.

Seity Y., P. Brousseau, S. Malardel, G. Hello, P. Bénard, F. Bouttier, C. Lac, and V. Masson, 2011, *The AROME-France Convective-Scale Operational Model*, *Monthly Weather Review*, Vol 139, pp976-991.

Sorteberg A., I. Haddeland, J. E. Haugen, S. Sobolowski, and W.K. Wong, (2014), *Evaluation of distribution mapping based bias correction methods*, *Norwegian Centre for Climate Services, NCCS report no.1/2014*.

Thiemeßl, M. J., A. Gobiet and A. Leuprecht, (2010), *Empirical-statistical downscaling and error correction of daily precipitation from regional climate models*, *Int. J. Climatology* DOI: 10.1002/joc.2168

Thiemeßl, M. J., A. Gobiet and G. Heinrich, (2012), *Empirical-statistical downscaling and error correction of regional climate models and its impact on the climate change signal*, *Climatic Change* 112: 449-468. DOI:10.1007/s10584-011-0224-4.

Tveito, O. E., and E. J. Førland. (1999), *Mapping temperatures in Norway applying terrain information, geostatistics and GIS*. *Norsk Geografisk Tidsskrift-Norwegian Journal of Geography* 53.4: 202-212.

Tveito, O. E., E. Førland, R. Heino, I. Hanssen-Bauer, H. Alexandersson, B. Dahlström, A. Drebs, C. Kern-Hansen, T. Jónsson, E. Vaarby-Laursen and Y. Westman, (2000) *Nordic temperature maps*. DNMI Report 09/00 KLIMA.

Tveito, O. E., et al. (2005) *A GIS-based agro-ecological decision system based on gridded climatology*. *Meteorological Applications* 12.1: 57-68.

Undén, P., Rontu, L., Järvinen, H., Lynch, P., Calvo, J., Cats, G., Cuaxart, J., Eerola, K., Fortelius, C., Garcia-Moya, J.A., Jones, C., Lenderlink, G., McDonald, A., McGrath, R., Navascues, B., Nielsen, N.W., Ødegaard, V., Rodriguez, E., Rummukainen, M., Rööm, R., Sattler, K., Sass, B.H., Savijärvi, H., Schreur, B.W., Sigg, R., The, H. and Tijm, A. (2002), *HIRLAM-5 Scientific Documentation, HIRLAM-5 Project*. Available from SMHI, S-601767 Norrköping, Sweden.

Uppala, S.M., Kållberg, P.W., Simmons, A.J., Andrae, U., da Costa Bechtold, V., Fiorino, M., Gibson, J.K., Haseler, J., Hernandez, A., Kelly, G.A., Li, X., Onogi, K., Saarinen, S., Sokka, N., Allan, R.P., Andersson, E., Arpe, K., Balmaseda, M.A., Beljaars, A.C.M., van de Berg, L., Bidlot, J., Bormann, N., Caires, S., Chevallier, F., Dethof, A., Dragosavac, M., Fisher, M., Fuentes, M., Hagemann, S., Hólm, E., Hoskins, B.J., Isaksen, L., Janssen, P.A.E.M., Jenne, R., McNally, A.P., Mahfouf, J.-F., Morcrette, J.-J., Rayner, N.A., Saunders, R.W., Simon, P., Sterl, A., Trenberth, K.E., Untch, A., Vasiljevic, D., Viterbo, P., and Woollen, J. (2005), *The ERA-40 re-analysis*. *Quart. J. R. Meteorol. Soc.*, 131, 2961-3012.

White and Toumi, 2013, *The limitations of bias correcting regional climate model inputs*, *Geophysical Res. Letters*, Vol. 40, 2907-2912, doi:10.1002/grl.50612.

5 Appendix

A1 MAPS

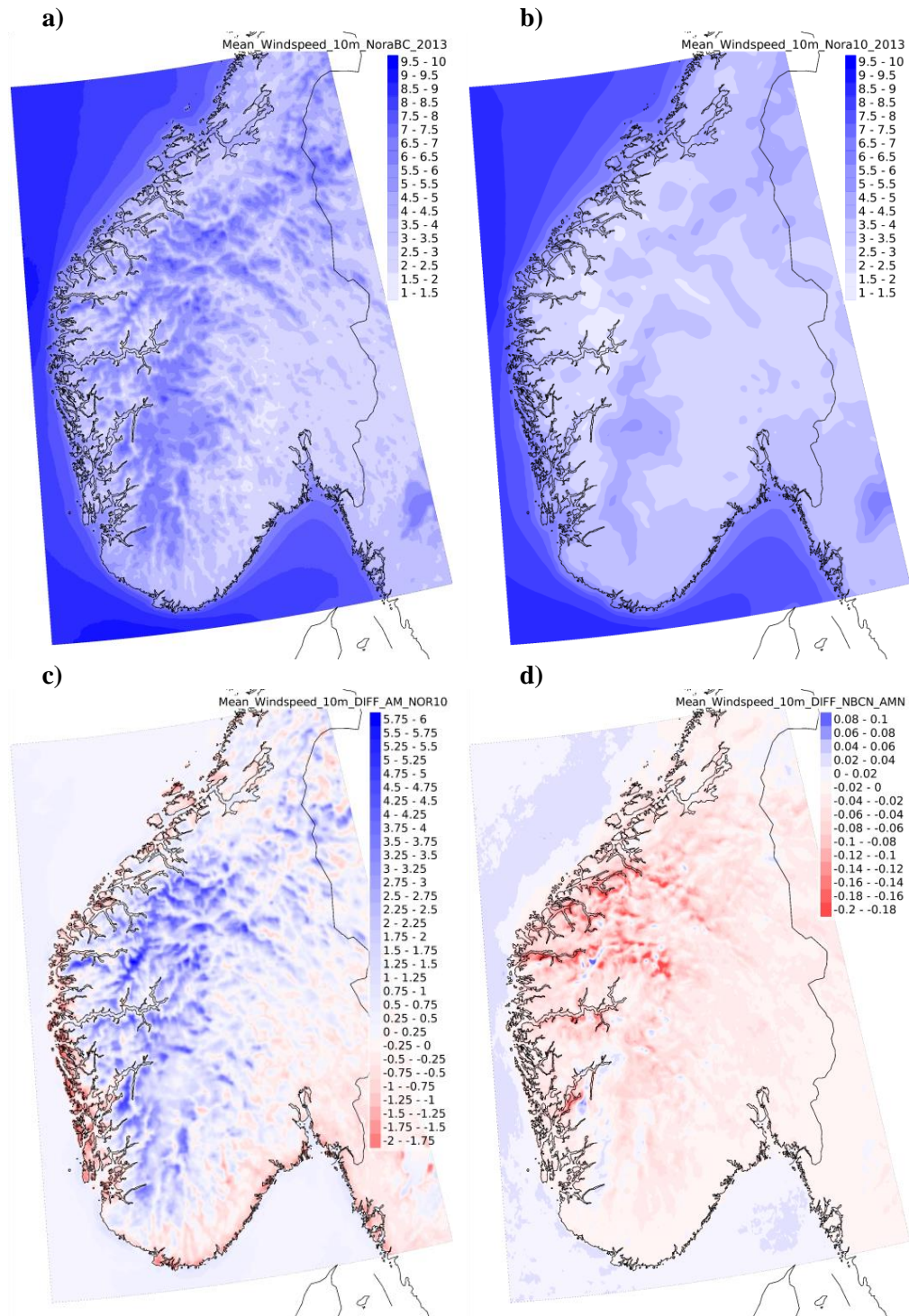


Figure A.1.1 10m wind speed [m/s].
 a) Mean of NORA-BC (2013),
 b) Mean of NORA10 (2013)
 c) The difference between AM2.5 and NORA10 (2013).
 d) The difference between NORA-BC (2000-2014) and AM2.5 (2013).
 a) b)

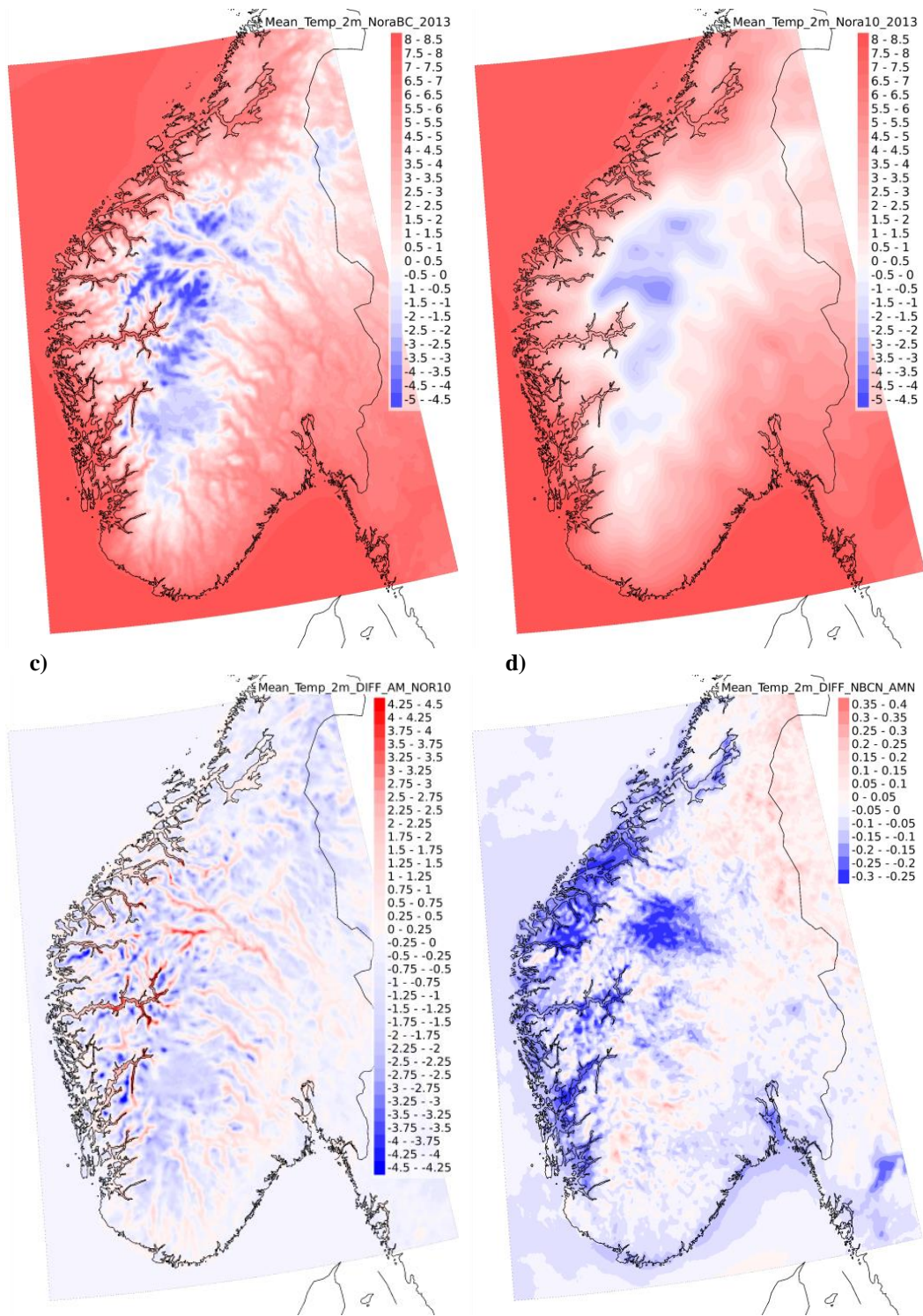


Figure A.1.2 2m temperature [°C] .
 a) Mean of NORA-BC (2013).
 b) Mean of NORA10-(2013).
 c) The difference between AM2.5 and NORA10 (2013).
 d) The difference between NORA-BC (2000-2014) and AM2.5 (2013).

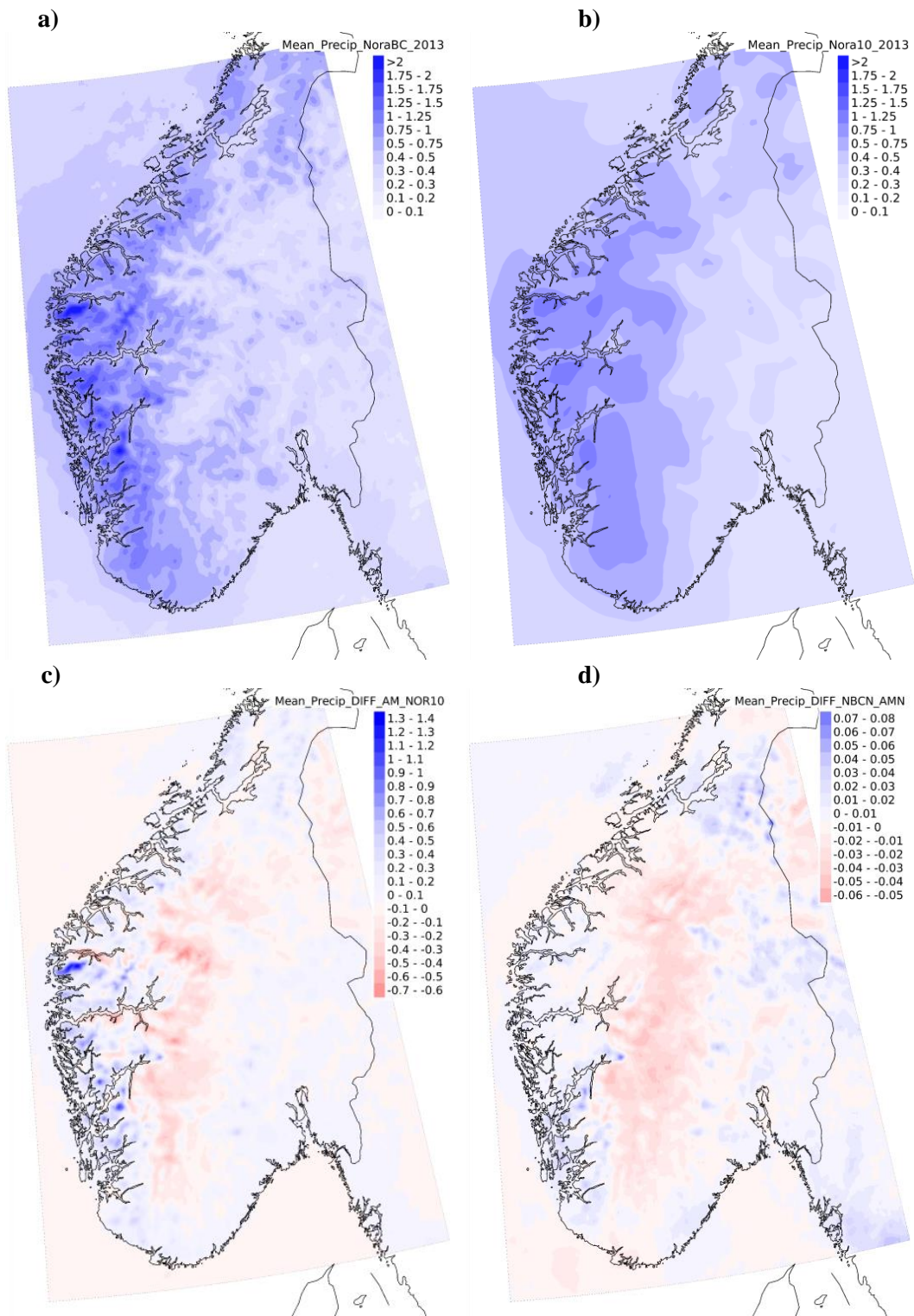


Figure A.1.3 3 hourly precipitation [mm/3 hours].
 a) Mean of NORA-BC (2013).
 b) Mean of NORA10 (2013).
 c) The difference between AM2.5 and NORA10. (2013).
 d) The difference between NORA-BC (2000-2014) and AM2.5 (2013).

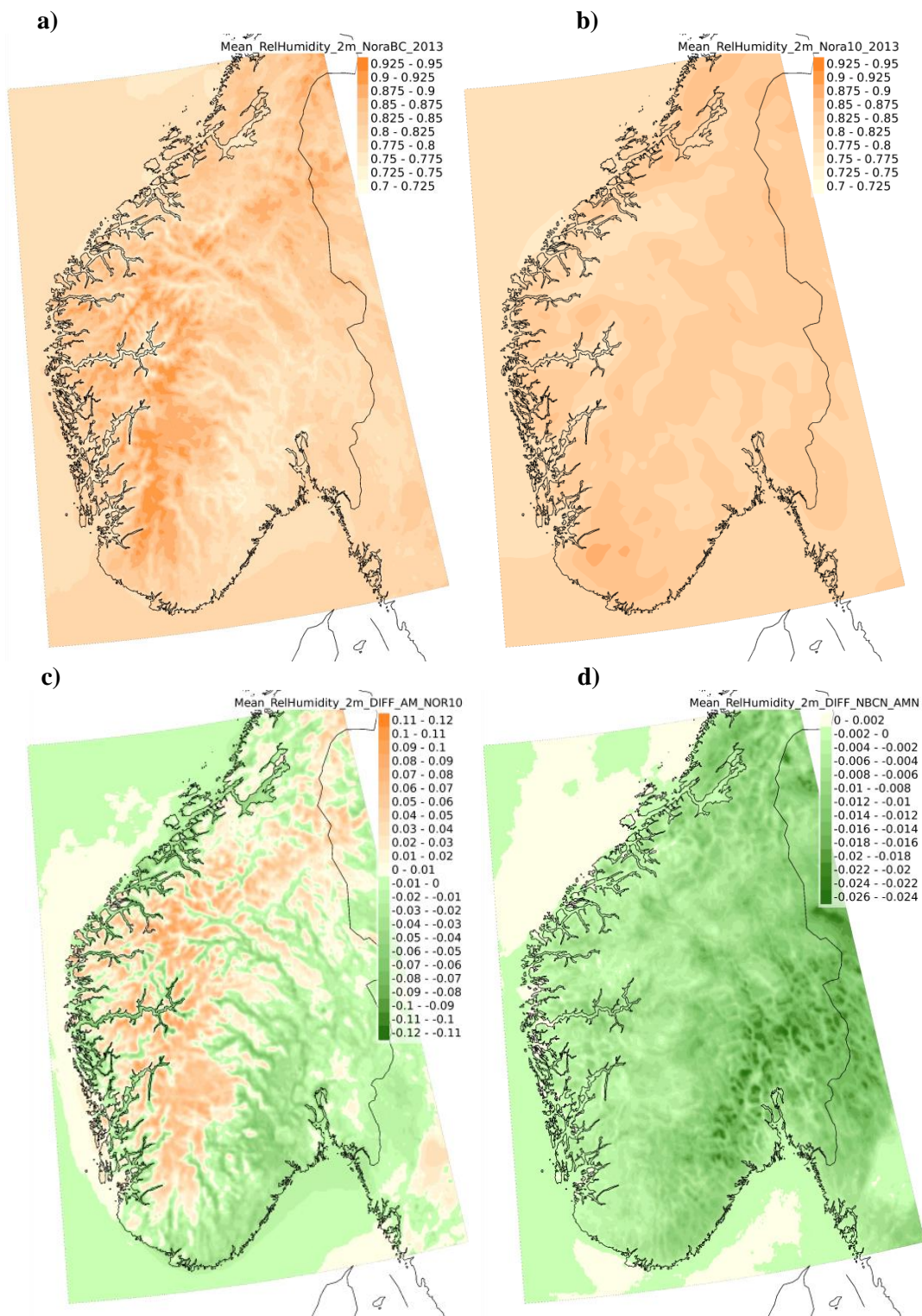


Figure A.1.4 2m relative humidity [0-1].
 a) Mean of NORA-BC (2013).
 b) Mean of NORA10 (2013).
 c) The difference between AM2.5 and NORA10 (2013).
 d) The difference between NORA-BC (2000-2014) and AM2.5 (2013).

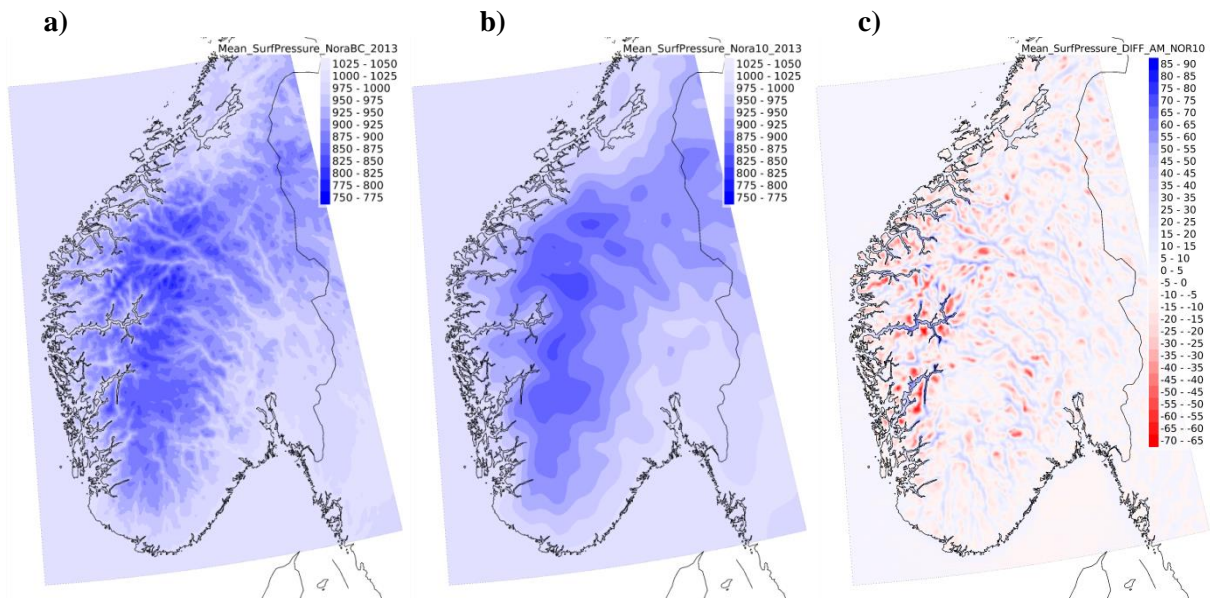


Figure A.1.5 Surface pressure [hPa].
 a) Mean of NORA-BC (2013).
 b) Mean of NORA10 (2013).
 c) The difference between AM2.5 and NORA10 (2013).

A2

Validation against observations

| | <u>WMO_NO; STNR; NAME;</u> | <u>LAT; LON</u> |
|-----|---|-----------------|
| 1. | 1203; 59110; KRÅKENES FYR; | 62.03; 4.98 |
| 2. | 1205; 59800; SVINØY FYR; | 62.33; 5.27 |
| 3. | 1209; 59680; ØRSTA-VOLDA; | 62.18; 6.07 |
| 4. | 1210; 60990; ÅLESUND_VIGRA; | 62.57; 6.12 |
| 5. | 1212; 62480; ONA; | 62.87; 6.53 |
| 6. | 1217; 62270; MOLDE; | 62.75; 7.27 |
| 7. | 1218; 60500; TAFJORD; | 62.23; 7.42 |
| 8. | 1220; 61410; MANNEN; | 62.46; 7.77 |
| 9. | 1223; 64330; KRISTIANSUND; | 63.10; 7.83 |
| 10. | 1228; 65940; SULA; | 63.85; 8.47 |
| 11. | 1230; 61630; BJORLI; | 62.26; 8.2 |
| 12. | 1232; 61420; MARSTEIN; | 62.45; 7.85 |
| 13. | 1238; 16610; FOKSTUA; | 62.12; 9.28 |
| 14. | 1239; 9310; HJERKINN II; | 62.22; 9.54 |
| 15. | 1240; 71850; HALTEN FYR; | 64.28; 9.70 |
| 16. | 1241; 71550; ØRLAND; | 63.70; 9.60 |
| 17. | 1245; 63705; OPPDAL - SÆTER; | 62.60; 9.67 |
| 18. | 1253; 67280; SOKNEDAL; | 62.95; 10.18 |
| 19. | 1254; 67560; KOTSØY; | 62.98; 10.56 |
| 20. | 1257; 68860; TRONDHEIM-VOLL; | 63.42; 10.45 |
| 21. | 1259; 71990; BUHOLMRÅSA FYR; | 64.40; 10.45 |
| 22. | 1265; 9580; TYNSET; | 62.27; 10.77 |
| 23. | 1271; 69100; VÆRNES; | 63.47; 10.93 |
| 24. | 1277; 71000; STEINKJER; | 63.72; 11.23 |
| 25. | 1278; 70150; VERDAL - REPPE; | 63.78; 11.67 |
| 26. | 1288; 10380; RØROS; | 62.57; 11.38 |
| 27. | 1290; 72580; NAMSOS LUFTHAVN; | 64.47; 11.58 |
| 28. | 1304; 57770; YTTERØYANE FYR; | 61.57; 4.68 |
| 29. | 1310; 57710; FLORØ LUFTHAVN; | 61.58; 5.03 |
| 30. | 1311; 50500; FLESLAND; | 60.30; 5.22 |
| 31. | 1317; 50540; BERGEN - FLORIDA; | 60.38; 5.33 |
| 32. | 1319; 52860; TAKLE; | 61.03; 5.38 |
| 33. | 1320; 58100; SANDANE; | 61.83; 6.12 |
| 34. | 1321; 58900; STRYN; | 61.88; 6.57 |
| 35. | 1322; 57420; FØRDE; | 61.47; 5.92 |
| 36. | 1323; 57000; FØRDE/BRINGELANDSÅSEN; | 61.40; 5.77 |
| 37. | 1329; 50070; KVAMSØY; | 60.35; 6.27 |
| 38. | 1337; 51530; VOSSEVANGEN; | 60.63; 6.43 |
| 39. | 1338; 53101; VANGSNES; | 61.17; 6.65 |
| 40. | 1347; 55700; SOGNDAL; | 61.25; 7.22 |
| 41. | 1350; 25830; FINSEVATN; | 60.60; 7.53 |
| 42. | 1360; 15730; BRÅTÅ - SLETTOM; | 61.90; 7.90 |
| 43. | 1361; 15890; GROTLI III; | 62.02; 7.66 |
| 44. | 1362; 15270; JUVVASSHØE; | 61.68; 8.37 |
| 45. | 1364; 54710; FILEFJELL - KYRKJESTØLANE; | 61.18; 8.11 |
| 46. | 1365; 23550; BEITOSTØLEN II; | 61.25; 8.92 |
| 47. | 1366; 55290; SOGNEFJELL; | 61.57; 8.00 |
| 48. | 1367; 23420; FAGERNES; | 60.98; 9.23 |
| 49. | 1368; 23410; FAGERNES LEIRIN; | 61.00; 9.30 |
| 50. | 1369; 23160; ÅBJØRSBRÅTEN; | 60.92; 9.29 |
| 51. | 1373; 24890; NESBYEN; | 60.57; 9.13 |
| 52. | 1375; 13160; KVITFJELL; | 61.50; 9.97 |
| 53. | 1376; 24710; GULSVIK II; | 60.38; 9.61 |
| 54. | 1378; 12680; LILLEHAMMER; | 61.08; 10.48 |
| 55. | 1380; 13420; VENABU; | 61.65; 10.12 |
| 56. | 1382; 12550; KISE; | 60.77; 10.80 |
| 57. | 1383; 8140; EVENSTAD; | 61.40; 11.15 |

| | | | | |
|-----|-------|--------------------------------|--------|-------|
| 58. | 1384; | 4780; GARDERMOEN; | 60.20; | 11.10 |
| 59. | 1389; | 7010; RENA; | 61.10; | 11.37 |
| 60. | 1392; | 6020; FLISA II; | 60.62; | 12.02 |
| 61. | 1393; | 700; DREVSJØ; | 61.88; | 12.05 |
| 62. | 1397; | 180; TRYSIL; | 61.50; | 12.45 |
| 63. | 1403; | 47300; UTSIRA FYR; | 59.30; | 4.88 |
| 64. | 1406; | 48330; SLÅTTERØY FYR; | 59.92; | 5.07 |
| 65. | 1407; | 48120; STORD LUFTHAVN; | 59.75; | 5.38 |
| 66. | 1408; | 47260; HAUGESUND; | 59.35; | 5.22 |
| 67. | 1415; | 44560; SOLA; | 58.88; | 5.63 |
| 68. | 1425; | 43010; UALAND - BJULAND; | 58.55; | 6.35 |
| 69. | 1427; | 42160; LISTA FYR; | 58.12; | 6.57 |
| 70. | 1433; | 46510; MIDTLÆGER; | 59.83; | 6.98 |
| 71. | 1434; | 33890; VÅGSLI; | 59.77; | 7.37 |
| 72. | 1436; | 41770; LINDESNES FYR; | 57.98; | 7.05 |
| 73. | 1439; | 41670; KONSMO - HÆGELAND; | 58.27; | 7.33 |
| 74. | 1441; | 40880; HOVDEN-LUNDANE; | 59.58; | 7.38 |
| 75. | 1448; | 39100; OKSØY FYR; | 58.07; | 8.05 |
| 76. | 1450; | 31620; MØSSTRAND II; | 59.85; | 8.07 |
| 77. | 1452; | 39040; KRISTIANSAND/KJEVIK; | 58.20; | 8.07 |
| 78. | 1455; | 37230; TVEITSUND; | 59.03; | 8.52 |
| 79. | 1459; | 36560; NELAUG; | 58.65; | 8.63 |
| 80. | 1465; | 36200; TORUNGEN FYR; | 58.38; | 8.8 |
| 81. | 1467; | 35860; LYNØR FYR; | 58.63; | 9.15 |
| 82. | 1469; | 20301; HØNEFOSS - HØYBY; | 60.17; | 10.25 |
| 83. | 1470; | 32060; GVARV - NES; | 59.38; | 9.20 |
| 84. | 1473; | 28380; KONGSBERG; | 59.62; | 9.63 |
| 85. | 1475; | 30420; GEITERYGGEN; | 59.18; | 9.57 |
| 86. | 1476; | 34130; JOMFRULAND FYR; | 58.87; | 9.60 |
| 87. | 1477; | 27010; KONNERUD; | 59.71; | 10.15 |
| 88. | 1480; | 26900; DRAMMEN - BERSKOG; | 59.75; | 10.12 |
| 89. | 1481; | 27450; MELSOM; | 59.23; | 10.35 |
| 90. | 1482; | 27500; FERDER FYR; | 59.03; | 10.53 |
| 91. | 1488; | 4460; HAKADAL JERNBANESTASJON; | 60.12; | 10.83 |
| 92. | 1490; | 18950; TRYVASSHØGDA; | 59.98; | 10.68 |
| 93. | 1492; | 18700; OSLO - BLINDERN; | 59.95; | 10.72 |
| 94. | 1493; | 3190; SARPSBORG; | 59.28; | 11.12 |
| 95. | 1494; | 17150; RYGGE; | 59.38; | 10.78 |
| 96. | 1495; | 17000; STROMTANGEN FYR; | 59.15; | 10.83 |

Table A2.1 Stations used in the analysis of 10m wind speed, 2m temperature and precipitation.

| | WMO NO; | STNR; NAME; | LAT; | LON |
|-----|----------------|--------------------|-------------|------------|
| 1. | 1205; | SVINØY FYR; | 62.33; | 5.27 |
| 2. | 1210; | ÅLESUND_VIGRA; | 62.57; | 6.12 |
| 3. | 1218; | TAFJORD; | 62.23; | 7.42 |
| 4. | 1241; | ØRLAND; | 63.70; | 9.60 |
| 5. | 1257; | TRONDHEIM-VOLL; | 63.42; | 10.45 |
| 6. | 1271; | VÆRNES; | 63.47; | 10.93 |
| 7. | 1311; | FLESLAND; | 60.30; | 5.22 |
| 8. | 1317; | BERGEN - FLORIDA; | 60.38; | 5.33 |
| 9. | 1319; | TAKLE; | 61.03; | 5.38 |
| 10. | 1369; | ÅBJØRSBRÅTEN; | 60.92; | 9.29 |
| 11. | 1382; | KISE; | 60.77; | 10.80 |
| 12. | 1384; | GARDERMOEN; | 60.20; | 11.10 |
| 13. | 1389; | RENA; | 61.10; | 11.37 |
| 14. | 1393; | DREVSJØ; | 61.88; | 12.05 |
| 15. | 1403; | UTSIRA FYR; | 59.30; | 4.88 |
| 16. | 1406; | SLÅTTERØY FYR; | 59.92; | 5.07 |
| 17. | 1415; | SOLA; | 58.88; | 5.63 |
| 18. | 1427; | LISTA FYR; | 58.12; | 6.57 |
| 19. | 1448; | OKSØY FYR; | 58.07; | 8.05 |

Table A2.2 Stations used in the analysis of long term trends (1960-2014) in 10m wind speed.

| | <u>WMO NO; STNR; NAME;</u> | <u>LAT; LON</u> |
|-----|------------------------------|-----------------|
| 1. | 1288, 10380, RØROS, | 62.57, 11.38 |
| 2. | 1375, 13160, KVITFJELL, | 61.50, 9.97 |
| 3. | 1361, 15890, GROTLI III, | 62.02, 7.66 |
| 4. | 1494, 17150, RYGGE, | 59.38, 10.78 |
| 5. | 1482, 27500, FERDER FYR, | 59.03, 10.53 |
| 6. | 1427, 42160, LISTA FYR, | 58.12, 6.57 |
| 7. | 1403, 47300, UTSIRA FYR, | 59.30, 4.88 |
| 8. | 1384, 4780, GARDERMOEN, | 60.20, 11.10 |
| 9. | 1311, 50500, FLESLAND, | 60.30, 5.22 |
| 10. | 1304, 57770, YTTERØYANE FYR, | 61.57, 4.68 |
| 11. | 1205, 59800, SVINØY FYR, | 62.33, 5.27 |

Table A2.3 Stations used in the analysis of wind direction.

| | | | |
|--------------------|------|----|----------|
| • Calm | 0.0 | -- | 0.3 m/s |
| • Light air | 0.3 | -- | 1.5 m/s |
| • Light breeze | 1.5 | -- | 3.3 m/s |
| • Gentle breeze | 3.3 | -- | 5.5 m/s |
| • Moderate breeze | 5.5 | -- | 8.0 m/s |
| • Fresh breeze | 8.0 | -- | 10.8 m/s |
| • Strong breeze | 10.8 | -- | 13.9 m/s |
| • Near gale | 13.9 | -- | 17.2 m/s |
| • Gale/Fresh gale | 17.2 | -- | 20.7 m/s |
| • Strong gale | 20.7 | -- | 24.5 m/s |
| • Storm/Whole gale | 24.5 | -- | 28.4 m/s |
| • Violent storm | 28.4 | -- | 32.6 m/s |
| • Hurricane force | 32.6 | -- | m/s |

Table A2.4 Beaufort wind scale.

| | |
|--------------------|--------------------------|
| • North | 348.75 – 11.250 degree |
| • North North-East | 11.250 – 33.750 degree |
| • North-East | 33.750 – 56.250 degree |
| • East North-East | 56.250 – 78.750 degree |
| • East | 78.750 – 101.250 degree |
| • East South-East | 101.250 – 123.750 degree |
| • South-East | 123.75 – 146.250 degree |
| • South South-East | 146.250 – 168.750 degree |
| • South | 168.750 – 191.250 degree |
| • South South-West | 191.250 – 213.750 degree |
| • South-West | 213.750 – 236.250 degree |
| • West South-West | 236.250 – 258.75 degree |
| • West | 258.750 – 281.250 degree |
| • West North-West | 281.250 – 303.750 degree |
| • North-West | 303.750 – 326.250 degree |
| • North North-West | 326.250 – 348.750 degree |

Table A2.5 Wind direction scale.

A2.1 10m Wind speed

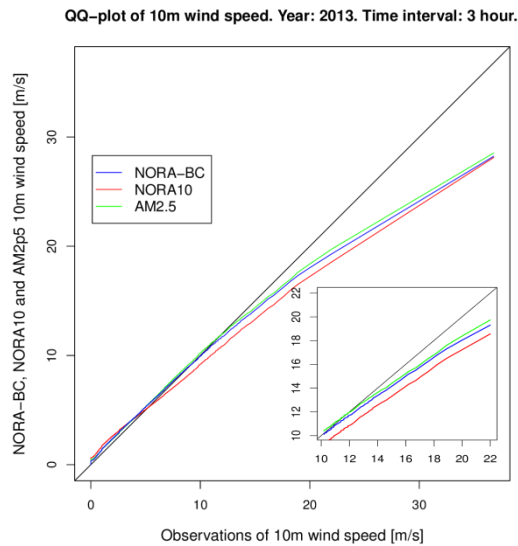


Figure A.2.1.1 QQ-plot of 10m wind speed.

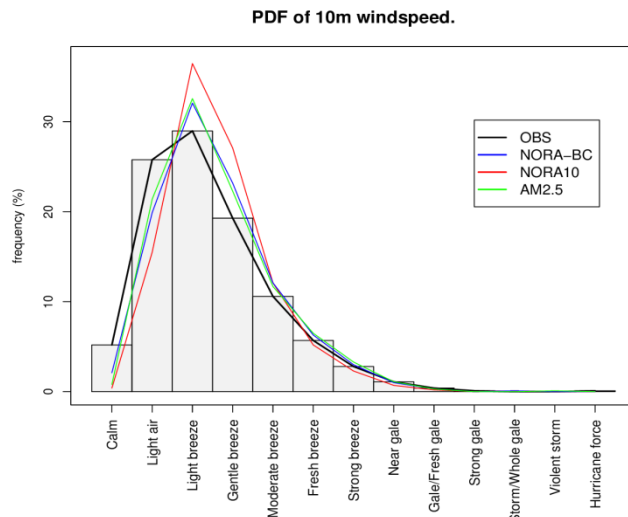


Figure A.2.1.2 PDF-plot of 10m wind speed.

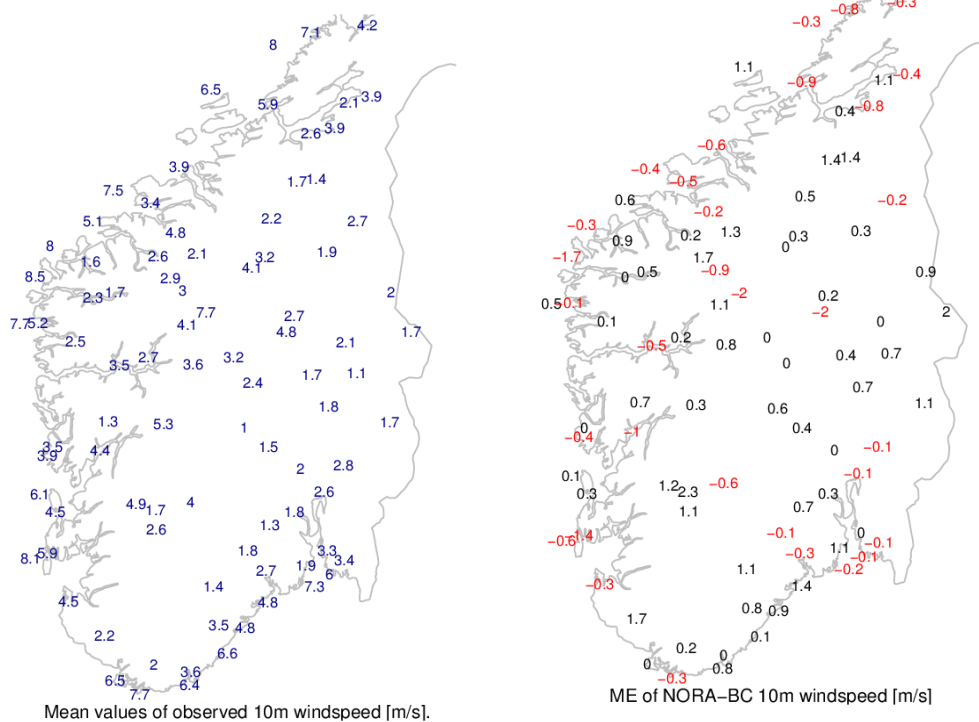


Figure A.2.1.3 a) Map showing mean values of observed 10m wind speed in the time period 2000 to 2014. b) Map showing the mean error in NORA-BC.

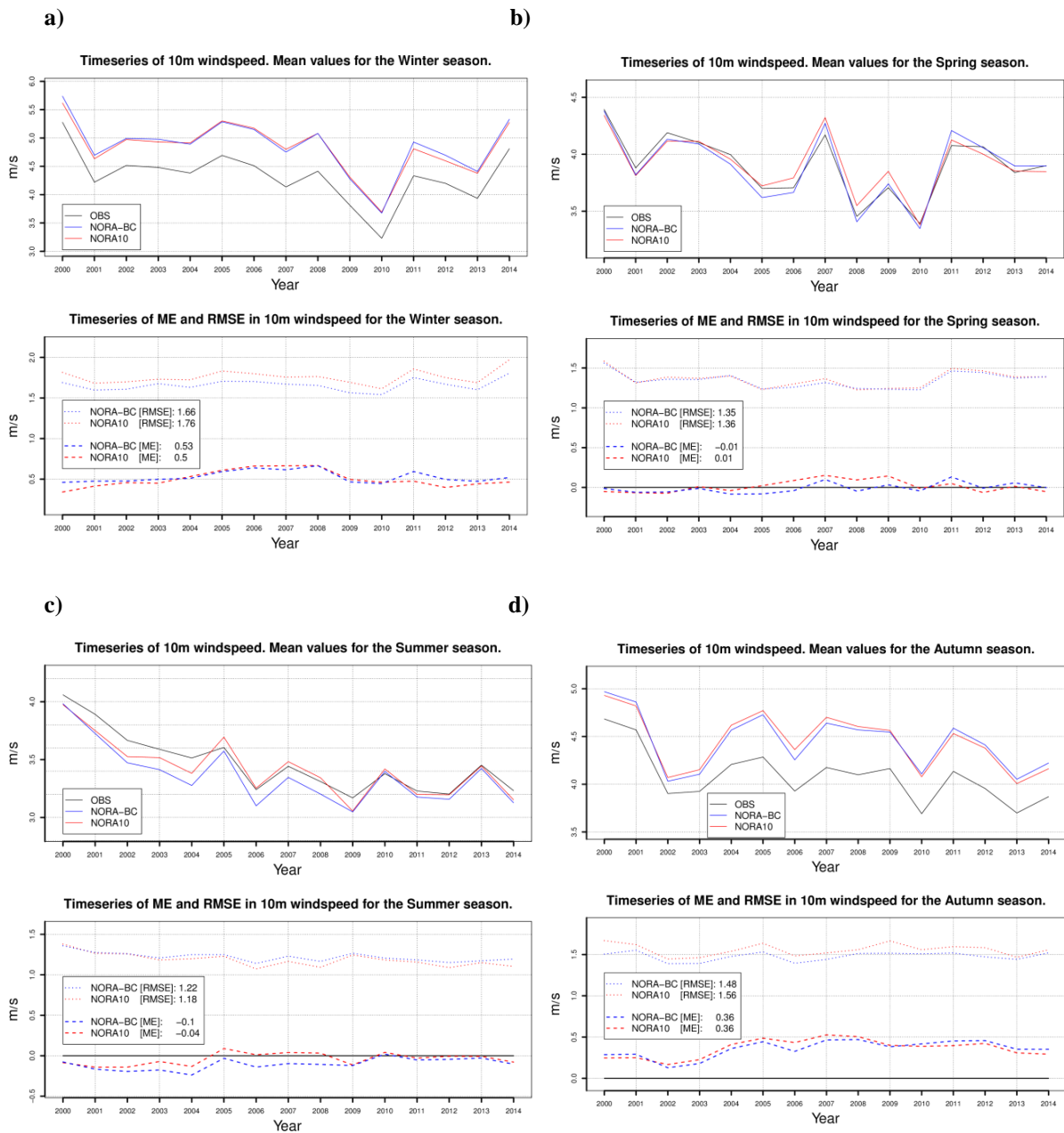
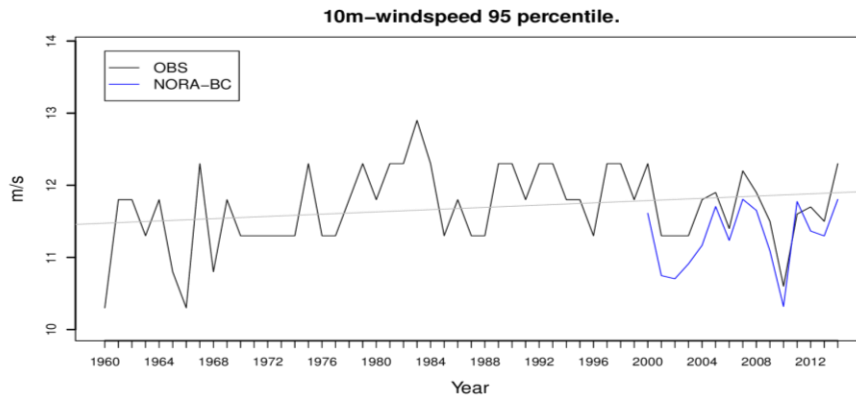
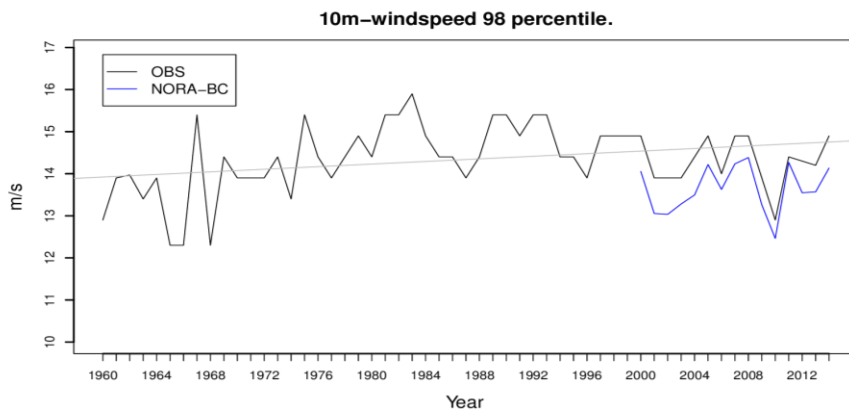


Figure A.2.1.4 Time series of 10m wind speed for the time period 2000-2014, divided into seasons (a-d). The black line is the mean value of the observations, the blue line is NORA-BC and the red line is NORA10. The uppermost figures show the mean values and the lowermost figures show mean errors and root mean square errors.

a)



b)



c)

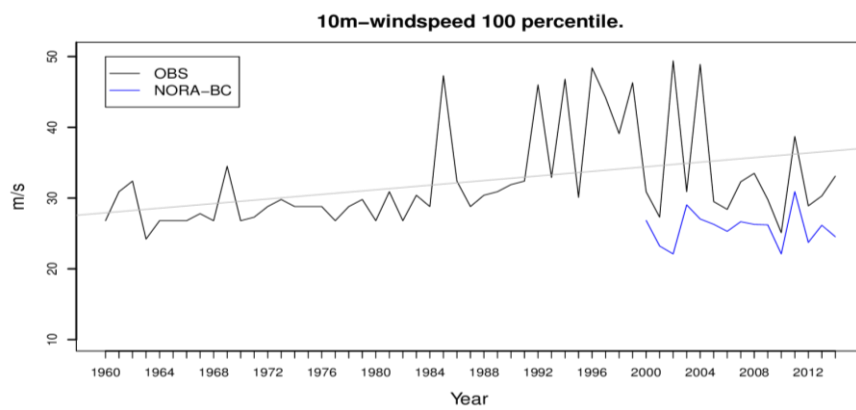


Figure A.2.1.5 Time series of the 95, 98 and 100 percentile (a-c) of 10m wind speed for the time period 1960-2014. The black line is the observations and the blue line is the NORA-BC.

A2.2 Wind direction in 10m above ground level.

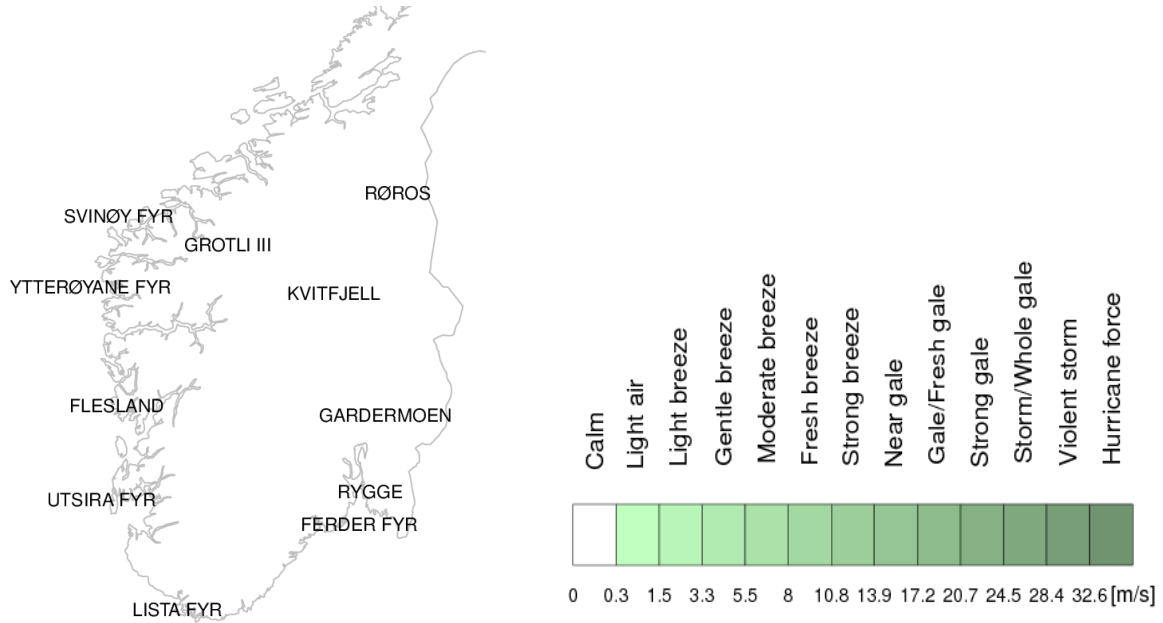
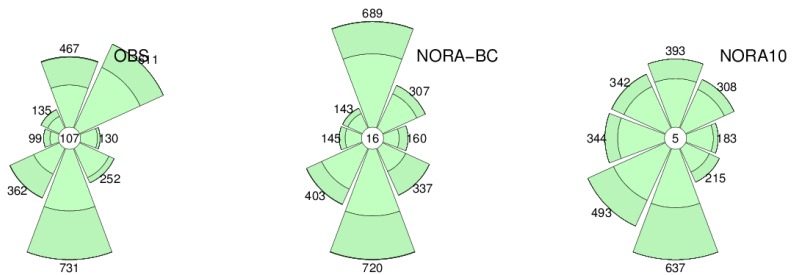


Figure A.2.2.1 Stations selected for wind direction analysis and the wind speed scale colour palette.

a)

GARDERMOEN

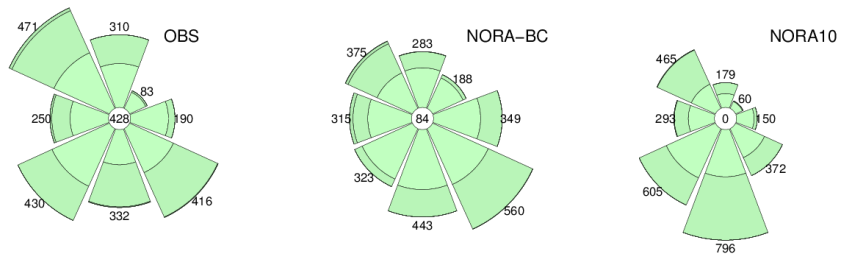
Time: 2013



b)

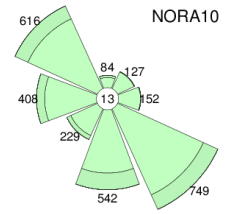
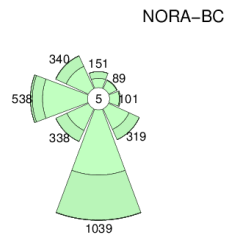
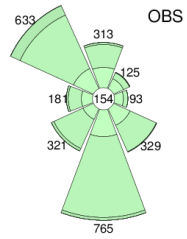
RØROS

Time: 2013



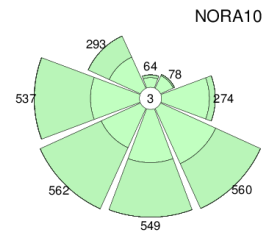
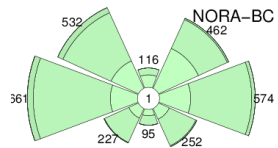
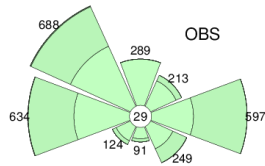
c)

KVITFJELL
Time: 2013



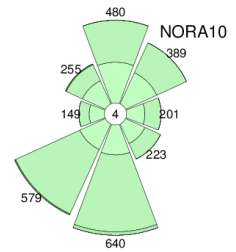
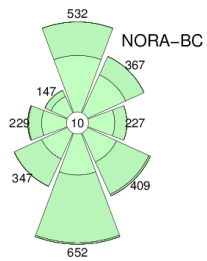
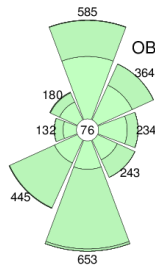
d)

GROTLI III
Time: 2013



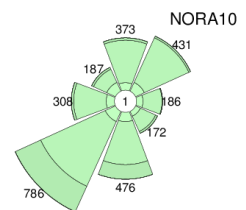
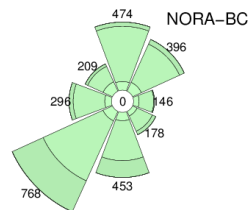
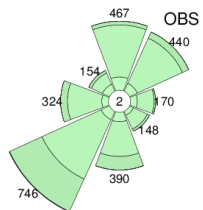
e)

RYGGE
Time: 2013



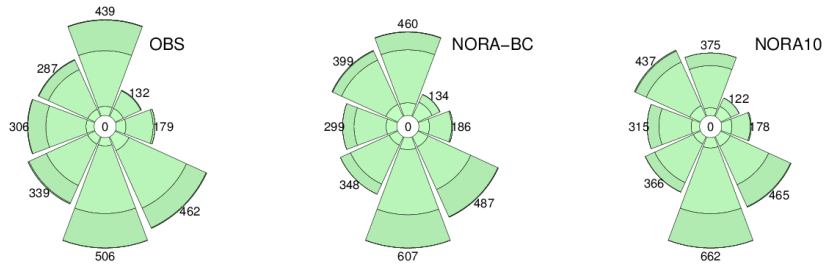
f)

FERDER FYR
Time: 2013



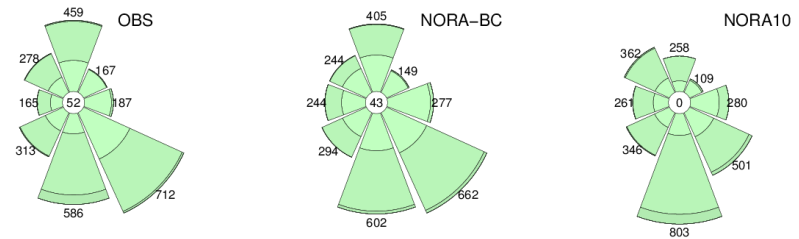
g)

UTSIRA FYR
Time: 2013



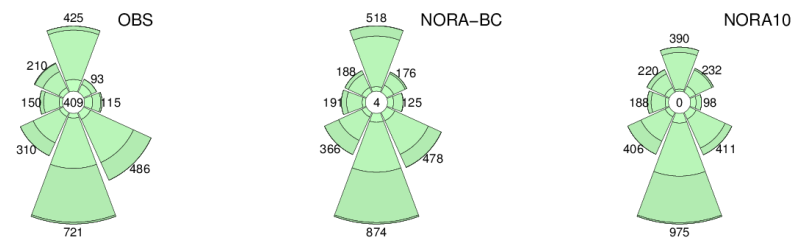
h)

FLESLAND
Time: 2013



i)

YTTERØYANE FYR
Time: 2013



j)

SVINØY FYR
Time: 2013

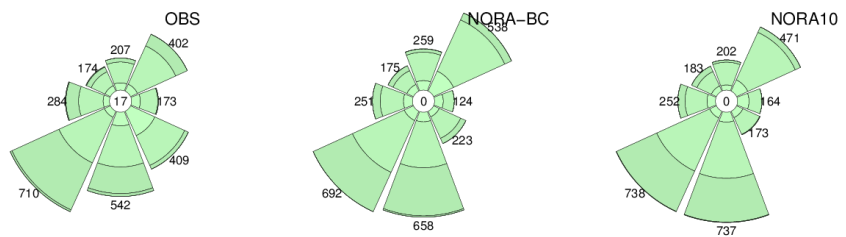


Figure A.2.2.2 Wind roses showing observed wind direction (OBS) and wind direction in NORA-BC and in NORA10. Each wind rose shows totally 2920 cases from the year 2013 when none of the observations are missing. The numbers represent the cases with wind from the specific direction. The number in the centre represents calm cases.

A2.3 Temperature 2m

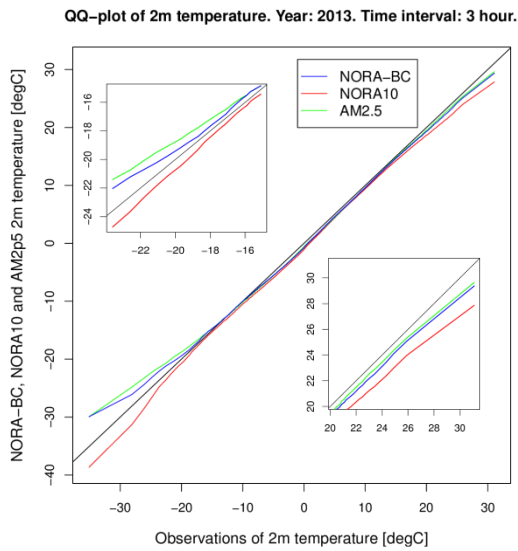


Figure A.2.3.1 QQ-plot of 2m temperature.

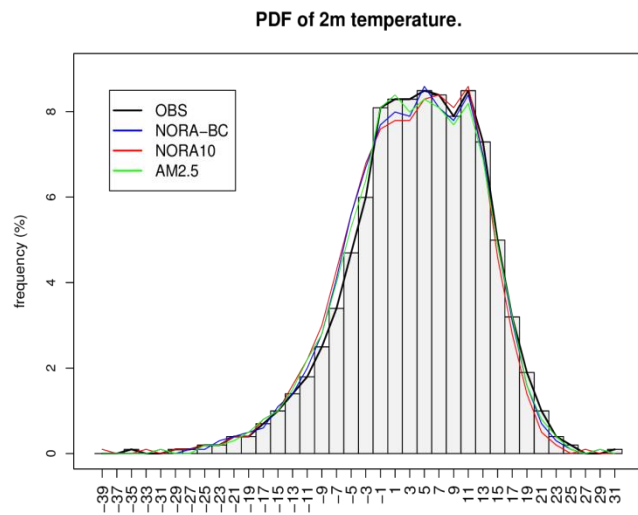


Figure A.2.3.2 PDF-plot of 2m temperature.

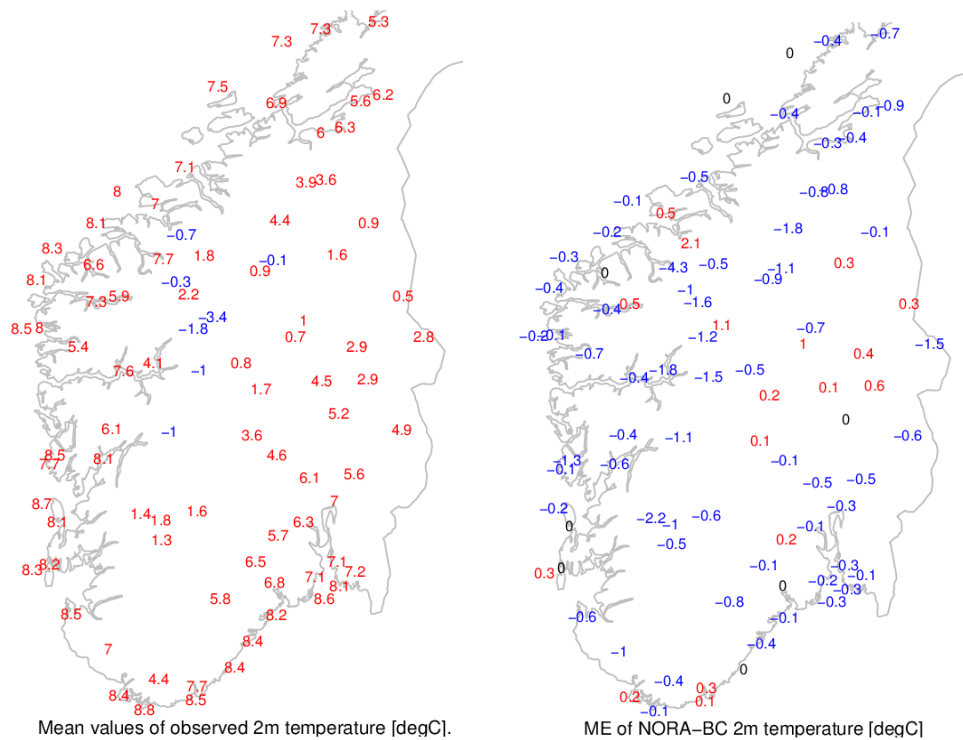


Figure A.2.3.3 a) Map showing mean values of observed 2m temperature in the time period 2000 to 2014. b) Map showing the mean error in the NORA-BC temperature.

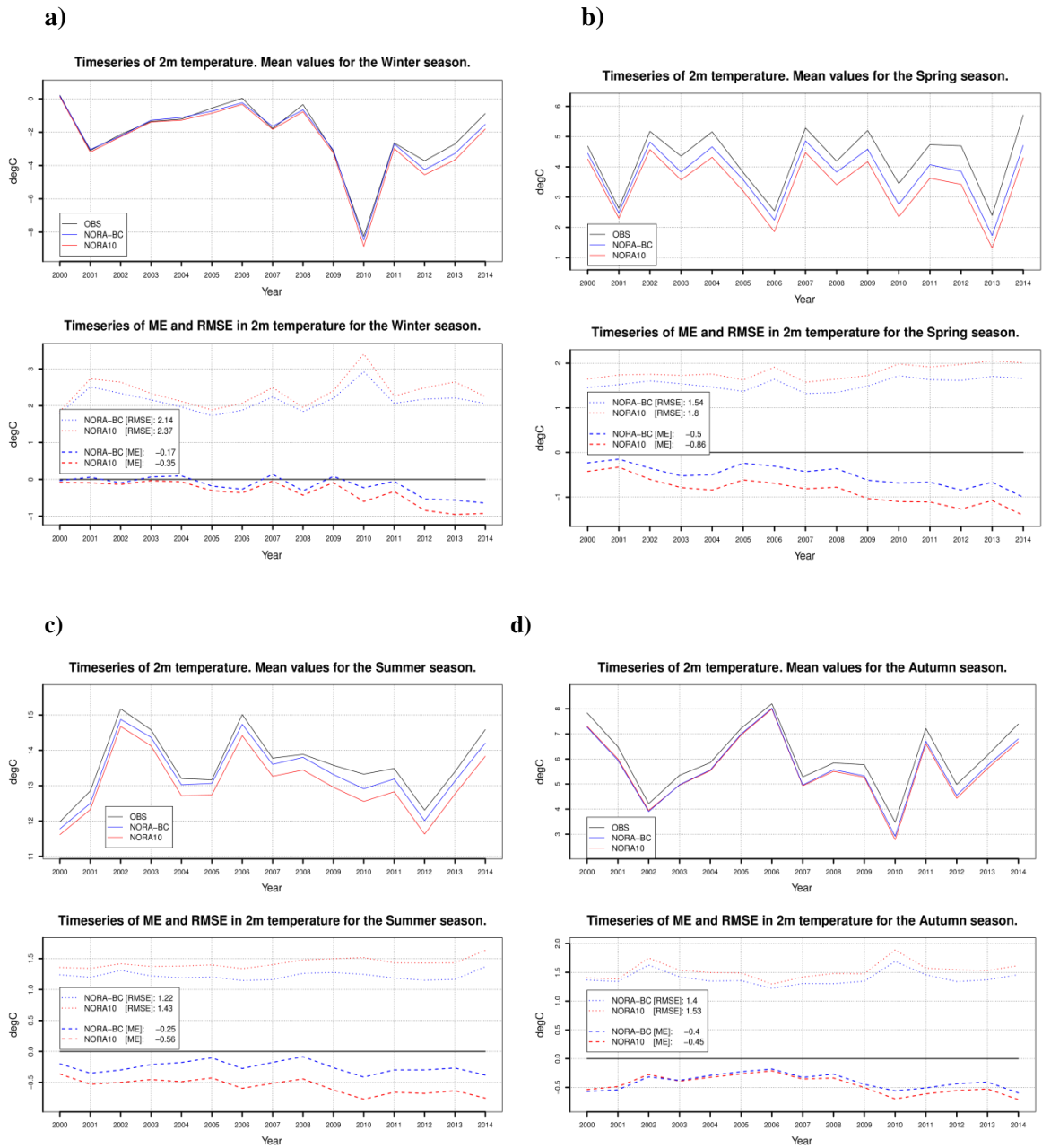


Figure A.2.3.4 Time series of 2m temperature for the time period 2000-2014, divided into seasons; a-d). The black line is the mean value of the observations, the blue line is NORA-BC and the red line is NORA10. The uppermost figures show the mean value and the lowermost figures show mean error and root mean square error.

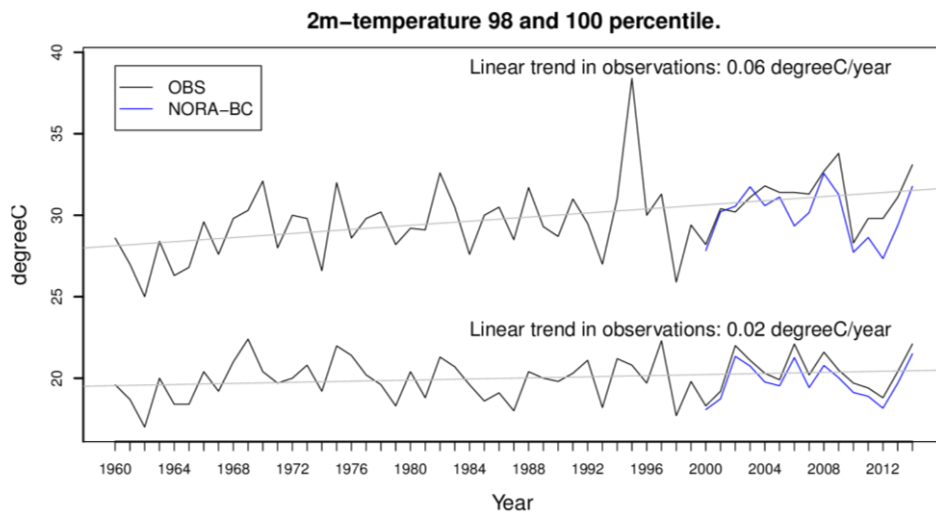


Figure A.2.3.5 Time series of the 98 and 100 percentile of 2m temperature for the time period 1960-2014.

A2.4 Three hourly precipitation

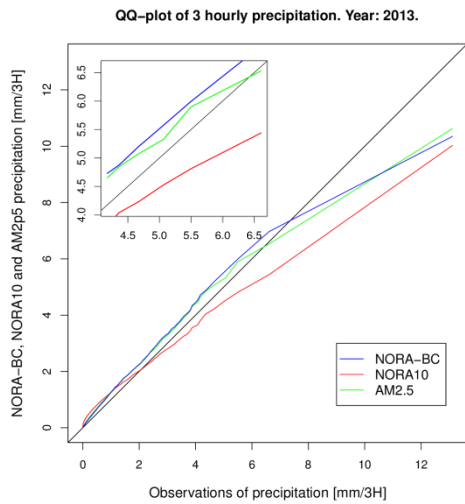


Figure A.2.4.1 QQ-plot of 3h precipitation.

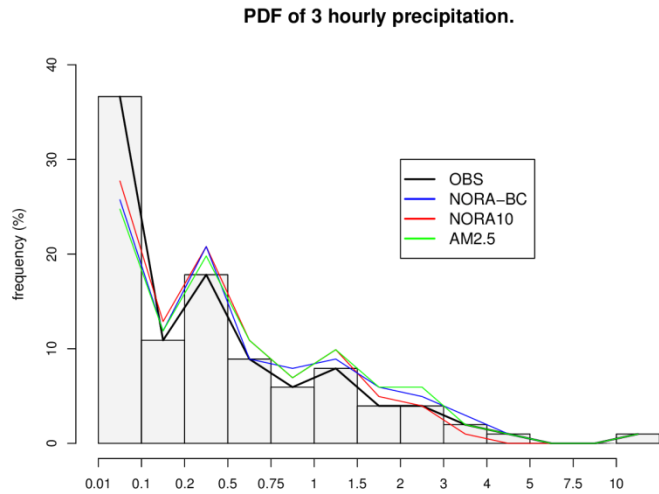


Figure A.2.4.2 PDF-plot of 3h precipitation

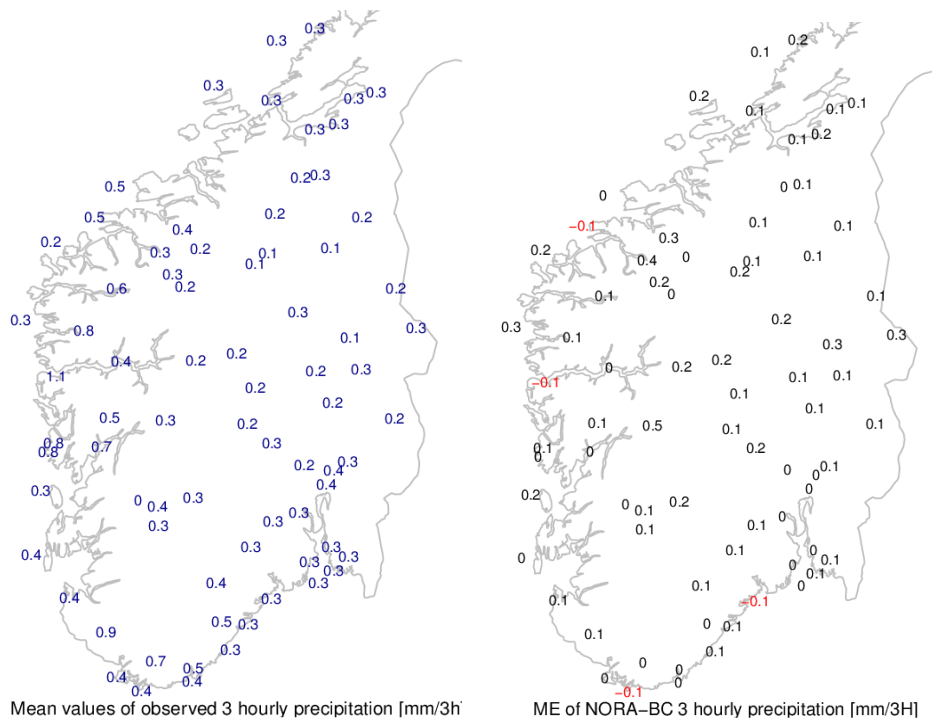


Figure A.2.4.3 a) Map showing mean values of observed precipitation [daily values/8] in the time period 2000 to 2014. b) Map showing the mean error in NORA-BC precipitation.

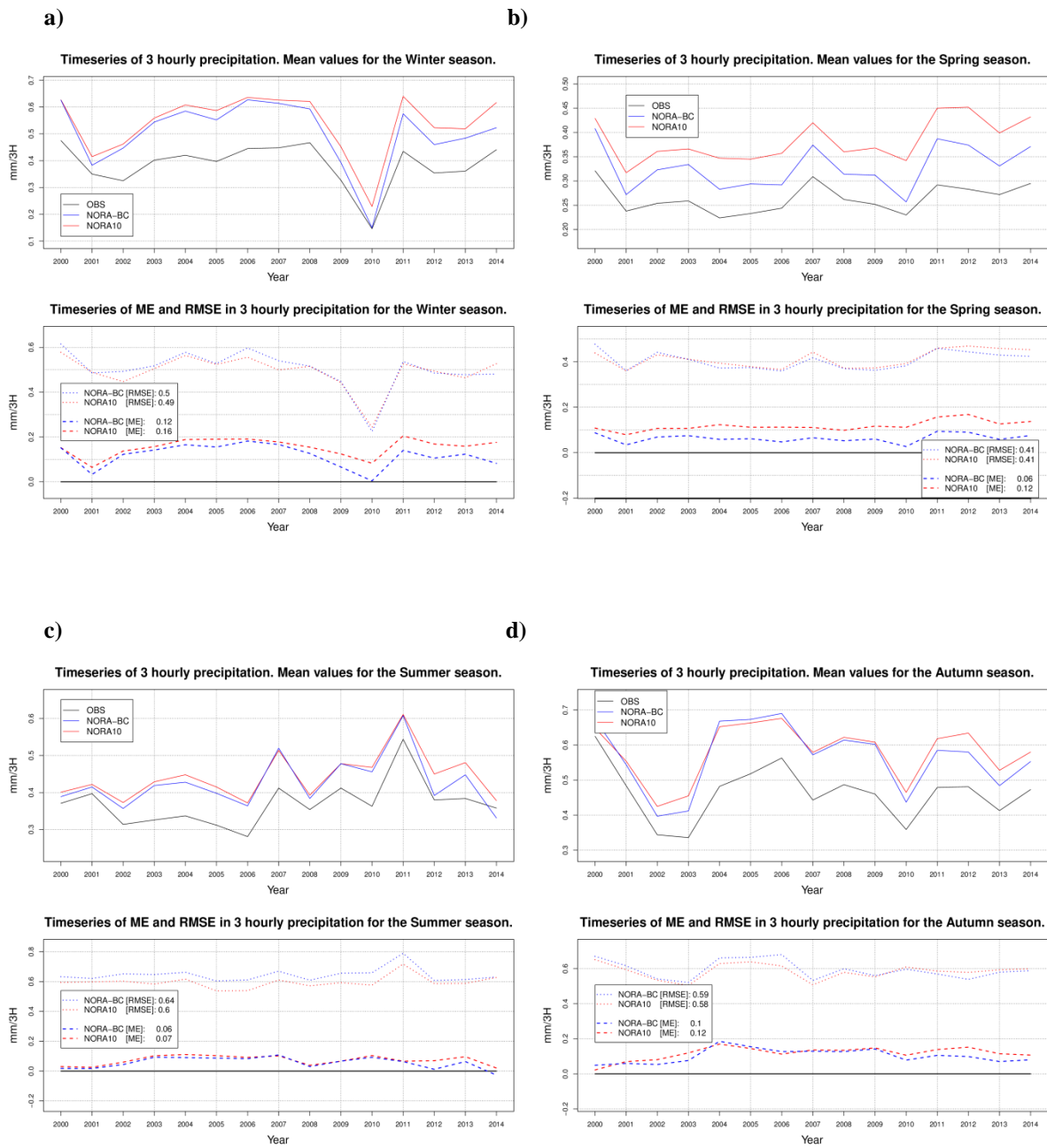


Figure A.2.4.4 Time series of 3 hourly precipitation for the time period 2000-2014, divided into seasons; a-d). The black line is the mean value of the observations, the blue line is NORA-BC and the red line is NORA10. The uppermost figures show the mean value and the lowermost figures show mean error and root mean square error.

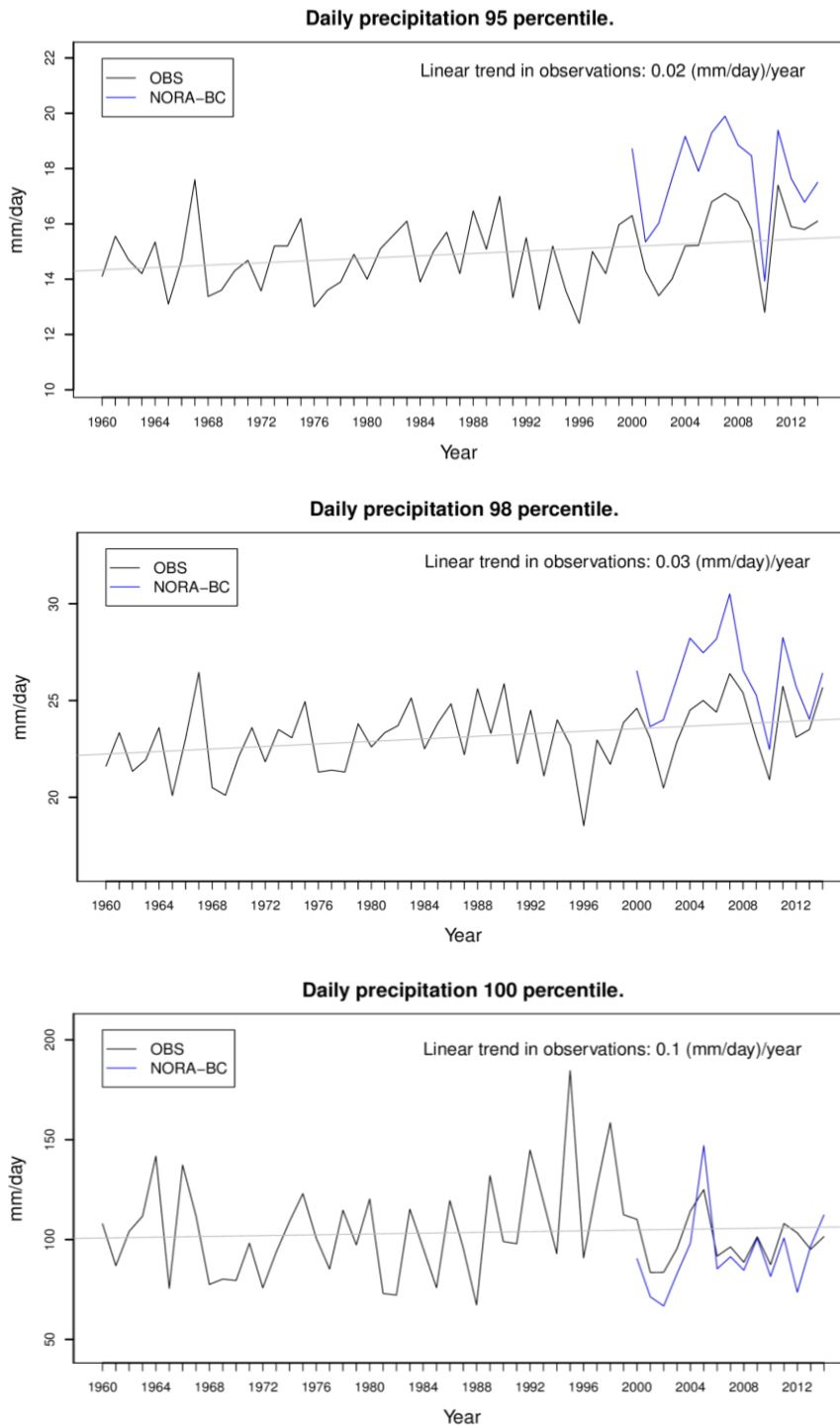


Figure A.2.4.5 Time series of the 95, 98 and 100 percentiles of daily precipitation for the time period 1960-2014, a-c). The black line is the observations, the blue line is NORA-BC.

A3 SeNorge fields

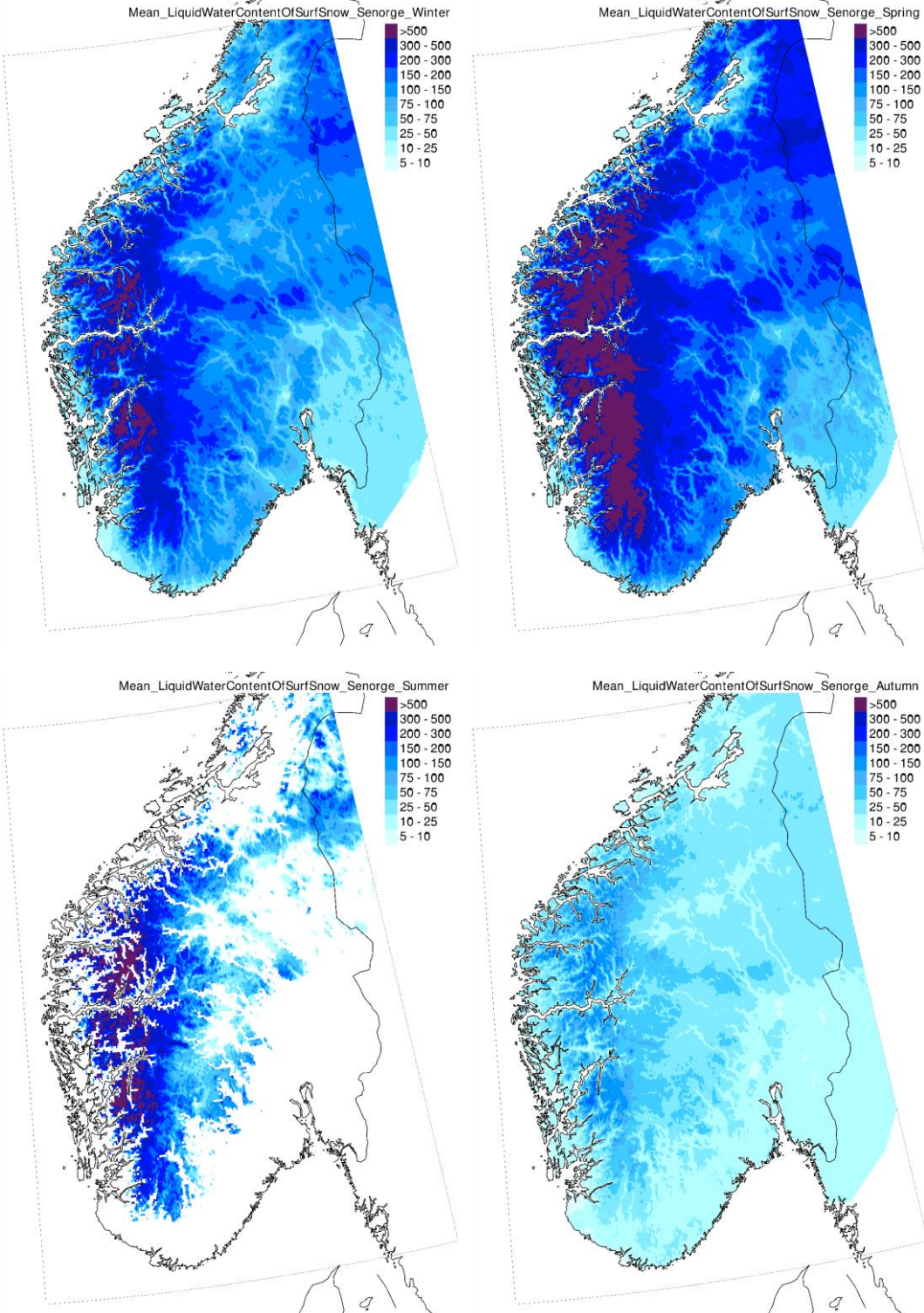


Figure A.3.1. The figure shows seasonal mean values of snow depth.

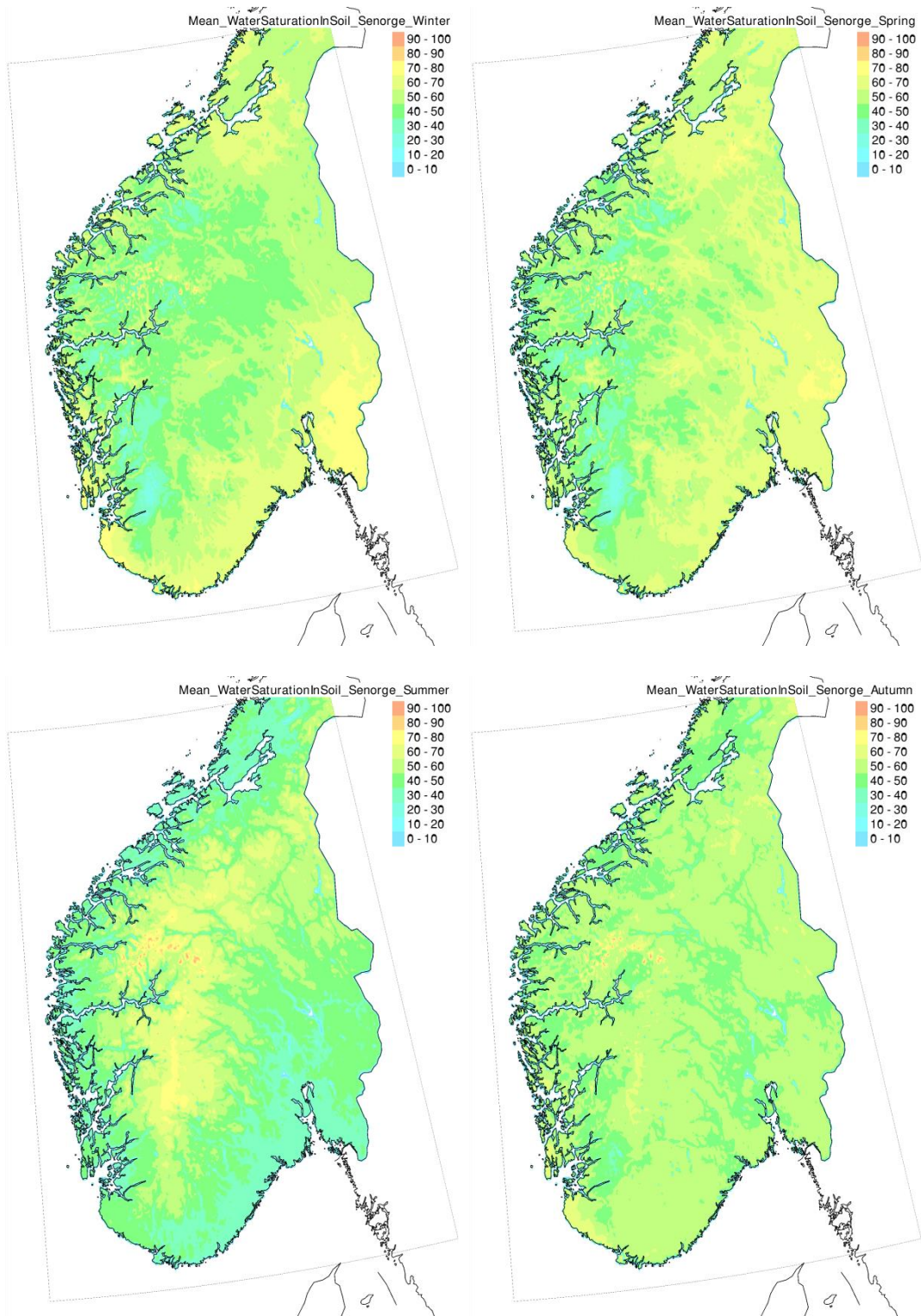


Figure A.3.2. The figure shows seasonal mean values of water saturation in soil.